Pressure-induced recovery of Fourier's law in one-dimensional momentum-conserving systems

Dye SK Sato[*]

Earthquake Research Institute, University of Tokyo, 1-1-1 Yayoi, Bunkyo, Tokyo 113-0032, Japan

We report the two typical models of normal heat conduction in one-dimensional momentum-conserving systems. They show the Arrhenius and the non-Arrhenius temperature dependence. We construct the two corresponding phenomenologies, transition-state theory of thermally activated dissociation and the pressure-induced crossover between two fixed points in fluctuating hydrodynamics. Compressibility yields the *ballistic* fixed point, whose scaling is observed in Fermi-Pasta-Ulam (FPU) β lattices.

I. INTRODUCTION

The microscopic root of macroscopic linear irreversible processes [1] has been closely studied through the research of heat conduction [2–4], where the processes are reduced to Fourier's law,

$$J = -\kappa \nabla T, \quad \kappa \propto N^0. \tag{1}$$

Here J, ∇T, κ, and N express energy currents, temperature gradients, heat conductivity, and the size of systems. The early works examined the connection between the relation that temperature gradient becomes the thermodynamic force ($J \propto \nabla T$) and the nonintegrability corresponding to phonon scattering [5–7]. Dimensionality is considered as an intrinsic factor for the intensive property of heat conductivity, e.g., *phonon localization* [8–10] and *anomalous heat conduction* [11]. The verification is still progressing [2,12–14].

Particularly, a universal breakdown of Fourier's law in one-dimensional momentum-conserving systems is supported by theories [11,15], numerical simulations [2,16–19], and experiments [20]. This systematic breakdown of the intensive property is called *anomalous heat conduction* and heat conductivity in these systems grows with the power of N,

$$\kappa \propto N^\alpha, \quad 0 < \alpha < 1. \tag{2}$$

This universality is described by a semimacroscopic continuum theory, *fluctuating hydrodynamic equations* [21], and the recent research [15,22–24] discovered its nontrivial relation with KPZ class, a broad class of dynamical critical phenomena [25]. The prediction of the theory and simulations clarified that α takes the universal value [11,15,17,19,22],

$$\alpha = 1/3. \tag{3}$$

The recent research also has deeply studied the scaling property of fluctuations and revealed the undoubted evidence of the connection that some scalings in these systems can be described by the KPZ equation [4,15,23,24,26]. Anomalous heat conduction forms the unique class connecting with KPZ class. Heat conductivity in one-dimensional momentum-conserving systems is considered to show the divergence in the thermodynamic limit.

The divergence of transport coefficients is considered as a general property of low dimensional momentum-conserving

systems and as the universal behavior of a fixed point in the fluctuating hydrodynamics [11,27–30]. If systems do not conserve momentum, they do not show such an anomaly [31–33]. As the ordinary understanding of anomalous heat conduction, the correlation function of spatially integrated energy currents $\hat{J}$ has the long time tails,

$$\frac{1}{N} \langle \hat{J}(0)\hat{J}(t) \rangle^{\text{eq}}_{T,P} \sim t^{\alpha-1}, \tag{4}$$

in $t_m \ll t < cN$ (t_m: microscopic characteristic time scale; c: sound velocity) [11,17,22,34], and it corresponds to the anomalous scaling. We used $\langle \rangle^{\text{eq}}_{T,P}$ as the isothermal isobaric equilibrium average. Equilibrium fluctuations of total energy currents $\hat{J}$ and heat conductivity are associated with a Green Kubo formula [35]

$$\kappa(T;P) = \lim_{N\to\infty} \frac{1}{NT^2} \int_0^\infty dt \langle \hat{J}(0)\hat{J}(t) \rangle^{\text{eq}}_{T,P}. \tag{5}$$

Recent research [15,24] clarified that the correlation of the heat mode, one of the plane waves in perfect fluids, contributes to the anomaly. The heat-mode autocorrelator $S_h(x,t)$ takes the asymptotic scaling form

$$S_h(x,t) \sim t^{-1/z} f_I(x/t^{1/z}). \tag{6}$$

f_I is the Levy distribution function. The exponent is another characterization of the fixed point,

$$z = 3/2. \tag{7}$$

Two exponents are connected with the dimension $d(\leqslant 2)$, e.g., through the renormalization-group approach [11] as $[z = 1 + d/2, \alpha = 1 - d/z(+0)]$. Even in the solids, the coefficient shows the divergence because of momentum conservation and dimensionality [20,30]. The anomaly has been studied mostly with the theory of fluids, but the mechanism is quite robust against such additional orders.

However, in spite of the completeness, the breakdown of this universality has been reported with recent detailed molecular dynamics [36–46]. The findings began with a model of polystable interaction potential energy, the coupled rotator model [36,37]. This model shows the convergence of heat conductivity at large sizes and has been studied to settle the unified sight between the anomaly and the *recovery of Fourier's law* [38]. Following it, the subsequent research has reported the abundant systems of the recovery [39–41]. The detailed investigation continues [42–46]. Some cases [39,40] were pointed out their finite size effects [42], but as the worst for the

───────
[*]dice@eri.u-tokyo.ac.jp

universality class, another report of the research [46] revealed that the diatomic hard-core systems can show the recovery in spite of the well-known feature as a paradigm of anomalous heat conduction. On the other hand, some authors [43] reported the possibility of the convergence caused by the quasistable *dissociation*. They also referred to the contributions of higher loop orders in fluctuating hydrodynamics, which was not studied in the previous analytical works. In the kinetic theory, the first foundation of the anomaly [27], such effects come from the deviation of the interactions from the description of the stochastic two body interactions (Boltzmann equations). So we may need the careful study of such many-body interactions, though they are thought to be the source of the anomaly. Actually, the quite recent research reported that the systems of multiparticle collisions showed the normal heat conduction [45]. One-dimensional momentum-conserving systems may form another class from the anomalous heat conduction. The unified view between the class of normal heat conduction and the ordinary anomalous class is far from established.

In this paper, we report the two different possibilities of the origin, thermally activated dissociation [43] and the increase of pressure. We first present the two typical models of normal heat conduction in one-dimensional momentum-conserving systems through the simulations of steady heat conduction. One shows the Arrhenius temperature dependence consistent with the previous work [43]. The other one shows the non-Arrhenius behavior. The latter suggests another mechanism of the convergence. Next we show that the latter one would be related to pressure through the observations of equilibrium current fluctuations. We try to explain the two mechanisms phenomenologically based on the transition-state theory of the dissociation formation and on the full fluctuating hydro-dynamic equations. In the latter analysis, the cutoff of the anomaly comes from the response to the pressure fluctuations. In the approach of mode coupling theory (MCT), one can see the convergence and a feature related to the breakdown of the hyperscaling between α and z. The renormalization group (RG) result suggests the recovery caused by the crossover between two fixed points. Compressibility yields the *ballistic* fixed point,

$$z = 1. \qquad (8)$$

We found that this scaling can be reproduced by the scaling discussions of the RG flows on full fluctuating hydrodynamic equations along the same procedure with [11]. The corresponding crossover is observed in the Fermi-Pasta-Ulam (FPU)-β lattices. Our results provide a picture of the recovery that the anomalous scaling can be cut off at N_*, the characteristic size of the dissociation or that of the crossover between the two fixed points,

$$\kappa \sim \begin{cases} N^\alpha, & N \ll N_* \\ N_*^\alpha, & N \gg N_*. \end{cases} \qquad (9)$$

The construction of this paper is as follows; First, in the Settings section, we set the system Hamiltonian and the two typical interaction potentials, and describe the details of two observations to measure the system-size dependence of heat conductivity. Next in the Results section, we report three results in the corresponding subsections: the first one

for steady heat conduction, the second one for equilibrium fluctuations of energy currents, and the third one for analysis. In the Discussion section, we discuss the correspondence of our results with the ordinary theories and with numerical simulations and the suggestion for experiments. We report the inviscid-ballistic scaling crossover of FPU-β lattices in the same section.

II. SETTINGS

A. Settings of systems

We study the one-dimensional N particle Hamiltonian systems of nearest-neighbor interactions,

$$\mathcal{H}(\Gamma) = \sum_{i=1}^{N} \left[\frac{p_i^2}{2m_i} + U(x_i) \right] + \sum_{i=1}^{N-1} V(x_{i+1,i}), \qquad (10)$$

with appropriate boundary conditions. $\Gamma :=$ $(x_1, \ldots, x_N, p_1, \ldots, p_N)$ is the phase space coordinate. With pinningless monatomic $[m_i = m, U(x) = 0]$, where the system should show the anomalous heat conduction, we set the two typical models of normal heat conduction. One is for thermally activated recovery, the pure repulsive-δ (PR-δ) model,

$$V(x) = \frac{g}{\delta} x^{-\delta}. \qquad (11)$$

The other is for pressure-induced recovery, the FPU-β model,

$$V(x) = \frac{K}{2} x^2 + \frac{\beta}{4} x^4. \qquad (12)$$

These two models show the different forms of temperature dependence on heat conductivity with each other. The former one suggests the noncontinuum mechanism as already reported in [43], and the latter one provides an inconsistent example with their class.

Pure repulsive δ is described here. The mechanical parameters are (m, g, δ, d, e). d is the average distance of particles given by the boundary conditions and e is the energy scale per particle given by the initial conditions or by attached thermostats. The free parameters are $[\delta, V_* := V(d)/e]$. x_i expresses the ith particle position. Two limits, $V_* \to 0$ (dilute high energy), ∞ (dense low energy), with finite δ correspond to integrable limits (of hard-core particles and of harmonic chains). This system shows the strong nonlinearity at $V_* \sim 1$. δ characterizes the interaction decay ($\delta \to 0$: log interactions, $\delta \to \infty$: hard core interactions). It has been already reported that this system should show the asymptotic convergence of heat conductivity at $\delta = 1, 6, 12$ [41]. Now we take the unit $(m, g) \to 1$ and choose the parameters as ($\delta = 6, V_* \sim 1$) to get the strong nonlinearity.[1]

FPU β has the following mechanical properties: (m, K, β, l, e) are the mechanical parameters of this system. l is

---

[1]In the sense that the maximum Lyapunov exponent is large compared with dilute case ($d > 1$) and the Lyapunov spectra shows the same shape with high energy FPU β, which correspond to the case that the Hessian of Hamiltonian is able to be replaced by the random matrix [47] on the surface spanned by conserved quantities.

the averaged compression given by the boundary conditions. e is the same with the PR-δ case. x_i expresses the deviation from the equilibrium point under the free boundary. An appropriate center uniquely determines it. The compression parameter l expresses the mismatch between the equilibrium position of force under the chosen boundary and that under the free boundary. We take the unit $(m, K, \beta) \to 1$. The left free parameters are (l, e) here. e decides the nonlinearity of the system ($e \to 0$: harmonic; $e \to \infty$: strong nonlinear), and l corresponds to the pressure. The heat conduction at $(e \gg 1, |l| \ll 1)$ is well studied [2], and it shows the fluctuating hydrodynamic (FH) scaling at large N [16,19]. Our simulations suggest the compression would be intrinsic for the recovery of Fourier's law. For the notation, we introduce the isodense potential (coordinate transformation $x_n \to y_n := x_n + nl$)

$$V(x) = \frac{K}{2}x^2 + \frac{\beta}{4}x^4 \to \frac{K}{2}(x-l)^2 + \frac{\beta}{4}(x-l)^4. \quad (13)$$

We call it compressed FPU β (c-FPU β) here. The isodense condition is tricky in FPU β (l-compressed fixed: $V(x_1) + V[-(N+1)l - x_N]$; l-compressed periodic: $V[x_1 - (x_N + Nl)]$), but easy in c-FPU β [fixed: $V(x_1) + V(-x_N)$; periodic: $V(x_1 - x_N)$]. We study its l dependence in the highly nonlinear regime ($e \gg 1$), where the system shows the FH anomaly at $l = 0$, zero pressure [16,19].

B. Settings of experiments

We studied two observables to investigate the system size dependence of heat conductivity. One is the heat conductivity defined by heat currents and temperature profiles under the states of steady heat conduction maintained by stochastic reservoirs. The other is power spectra of total energy currents under the isolated equilibrium conditions with periodic boundaries. We note that we studied heat conductivity of the former case under the globally far from equilibrium conditions where the temperature difference of the attached reservoirs is comparable with the average temperature of them. If the system recovers the intensive property of heat conductivity, this observation lets us see the temperature dependence of the heat conductivity under the isobaric conditions. The temperature dependence connects to the possible mechanisms of the recovery. As an example, the dissociation class shows the Arrhenius temperature dependence of heat conductivity [43].

The details of time integrations and of reservoirs are as follows. We use the fourth order symplectic integrator with time steps $\Delta t = 0.0025$ in PR-6 and with $\Delta t = 0.02$ in c-FPU β. We also checked the independence of our results on time steps by the changing $\Delta t \to \Delta t/4$ in some experiments. For PR-6, we set the thermal wall boundaries [17] at both edges ($x = 0, Nd$). For c-FPU β, we introduce the potential boundaries [$V(x_1) + V(-x_N)$] and attach the boundary reservoirs of Langevin type (viscosity: γ) to the $10 + 10$ particles at the corresponding edges. The algorithm of the attachment is geometric Langevin type [48]. The reservoir parameters are chosen as $(T_L, T_R, d) = (4, 1, 3/4)$ for PR-6 and $(T_L, T_R, \gamma) = (50, 30(10), 2)$ for c-FPU β. We make the initial conditions with the attachment of Langevin reservoirs in equilibrium cases.

III. RESULTS

A. Result of nonequilibrium simulation

1. Definitions of temperature and heat conductivity

We also note about the arbitrariness of the defined heat conductivity. One can define energy currents and temperature profiles based on the particle index or on the field coordinate [3]. This is a property of the lattice systems. This arbitrariness makes the following confusing situations under the globally far from equilibrium conditions. The density heterogeneity causes the two different temperature gradients, although the steady state values of the energy currents show the quantitative correspondence ($\langle J_{\text{field}} \rangle = \langle J_{\text{particle}} \rangle$ for PR-6). Then the values of heat conductivity defined by the ratios are different. This difference remains even though the system is of nearly local equilibrium, because the system satisfies the isobaric (not isodense) conditions under the steady heat conduction. In our PR-6 case, however, we observe that the density difference takes a rather small value, roughly 10% of initial packing density d^{-1}. This is negligible for the discussion of the anomaly. In the compressed FPU-β case there is no arbitrariness, because one can take the lattice constant as large as one wants [19]. We take the particle type observables, e.g., $J_{n+1,n} := \frac{p_{n+1} + p_n}{2}(-\frac{\partial V(x_{n+1,n})}{\partial x_{n+1,n}})$ with energy density $e_n := p_n^2/(2m) + [V(x_{n+1,n}) + V(x_{n,n-1})]/2$, through this paper. One can also define the stress along particle coordinates $\sigma_{n+1,n} = -\frac{\partial V(x_{n+1,n})}{\partial x_{n+1,n}}$. It gives the pressure of the steady state (in the sense of particle coordinates) conforming to the virial theorem.

Now we observe the kinetic temperature, which corresponds to the thermodynamic one under the local equilibrium condition [$(T_{n+1} - T_n)/T_n \ll 1$ for the finite interparticle distance]. Here, the kinetic temperature is defined as

$$T_n := \left\langle \frac{p_n^2}{m_n} \right\rangle. \quad (14)$$

We use the bracket $\langle \rangle$ to express the long time average.

Figure 1 is the temperature profile of c-FPU β under the steady heat conduction at $(T_L, T_R, l, N) = (50, 10, 4, 2^{15})$ and shows the gaps at the edges and the gradient varying at the bulk. As N increases, the gaps are slowly decreasing and the
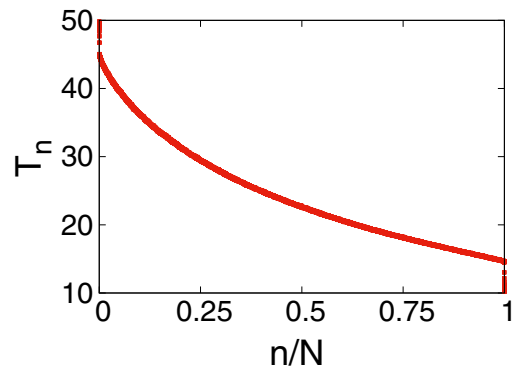

FIG. 1. The temperature profile of c-FPU β at $(T_L, T_R, l, N) = (50, 10, 4, 2^{15})$. One can see the gaps and the varying gradient.
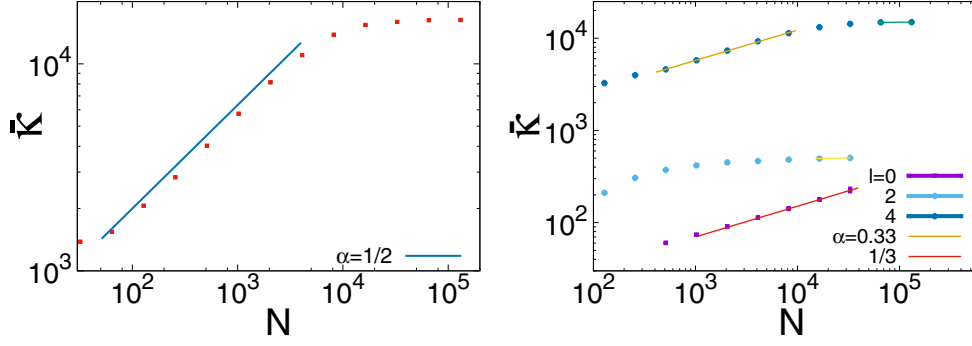
FIG. 2. Bulk heat conductivity (left: PR-6; right: c-FPU β). Parameters are $(T_L, T_R, d) = (4, 1, 3/4)$ for PR-6 and $(T_L, T_R, \gamma, l) = (50, 30, 2, 4)$ for c-FPU β. They show the convergence except c-FPU β at $l = 0$. The transient exponents are $1/2$ in PR-6 and 0.33 in c-FPU β at $l = 4$. For accuracy, we check the power of the last two points in c-FPU β at $l = 2, 4$ as an indicator of the convergence. The powers are $0.018(l = 2)$ and $0.009(l = 4)$, which show the quantitative evidence of the convergence.

varying gradient remains.[2] The situation of the PR-6 case is the same with it. We consider the points. First, it is necessary to remove the boundary gap, which can show the convergence of pretense [17], for the accurate observation of the system size dependence. Second, the spatially varying gradient means the spatially varying heat conductivity.

Then we define heat conductivity in two ways to discuss its system size dependence and its spatial variance. $J_{n+1,n}$ is independent of the index in the average of the steady state if the $n, n + 1$th particles have no interaction with reservoirs. So we simply call it J. First, to study the system size dependence, we introduce the bulk averaged gradient $\overline{\nabla_n T_n}$, which is given by the linear fitting of T_n in $1/4 \leqslant n/N \leqslant 3/4$, and define the following heat conductivity:

$$\bar{\kappa}(N) := \langle J \rangle / \overline{\nabla T}. \tag{15}$$

Here we call it bulk heat conductivity. We discuss the anomaly of the bulk through this observable under an assumption that the effect of the discontinuities is negligible. This assumption is valid in nonintegrable large systems. These gaps occur within the reservoir-attached particles at the edges, so they come from purely interfacial resistance. Second, to study the spatial variance, we introduce the segmented averaged gradient $\widehat{\nabla_n T_n}$, which is given by the linear fitting of T_n in a sufficiently narrow temperature range sufficiently slowly varying, and define the following heat conductivity with the assumption that $\widehat{\nabla_n T_n}$ is a function of the average temperature of each segment and N,

$$\kappa(T; N) := \langle J \rangle / \widehat{\nabla T}. \tag{16}$$

Now we call it local heat conductivity. We took two ways to prepare the data of such a temperature range. One is that we equally divide the data 16 (or 32) and cut out T_n of the reservoir-attached particles. The other is that we set $(T, \Delta \ll T)$ and extract T_n satisfying the condition $|T_n - T| < \Delta$. Our assumption of local heat conductivity is valid in the systems of normal heat conduction. Heat conductivity of normal heat conduction depends only on the local thermodynamic quantities,

although that of anomalous heat conduction depends also on the positions and on the system sizes. Then, this observable lets us know the temperature dependence of the heat conductivity under the isobaric conditions of the pressure P given by the boundary conditions, if the system recovers the intensive property of heat conductivity. We study the asymptotic master curve of the intensive heat conductivity. We can observe such temperature dependence at once under the globally far from equilibrium conditions.

2. System size dependence of bulk heat conductivity

Figure 2 is the result of the bulk heat conductivity $\bar{\kappa}$ and shows the convergence in some ways. $\bar{\kappa}$ of PR-6 shows the transient anomalous scaling $\alpha = 0.498 \pm 0.005$ in $10^2 \lesssim N \lesssim 10^4$ (the exponent of which is fitted in $2^7 \leqslant N \leqslant 2^{12}$) and the recovery of normal heat conduction without showing the FH scaling $\alpha = 1/3$. $\bar{\kappa}$ of c-FPU β is somewhat strange. It shows the FH anomalous scaling $\alpha = 1/3$ at $l = 0$, consistent with previous reports [16,19], but it shows the convergence at $l = 2, 4$. Particularly, at $l = 4$, it shows the anomalous scaling $\alpha = 0.330 \pm 0.006$ in the transient N dependence (fitted in $2^9 \leqslant N \leqslant 2^{13}$), which is almost the FH exponent $1/3$. It suggests that the convergence should occur after the FH scaling, in the continuum limit.

$\bar{\kappa}$ of PR-6 shows the divergence with the exponent $\alpha \simeq 1/2$ in $10^2 \lesssim N \lesssim 10^4$ and the convergence at larger sizes. This convergence is consistent with [43]. Its exponent $\alpha \simeq 1/2$ is larger than FH scaling $\alpha = 1/3$ and just the second universality exponent [49,50]. The intensive behavior remains even at $N \sim 10^5$. As recently reported, diatomic hard core shows the convergence if their chosen parameters are nearly integrable [46]. Some nearly integrable systems may show significant slowdown to obey the prediction of the continuum theory like in the FPU problem [15]. However, our choice of parameters provides the strong nonlinearity, although PR-6 has integrable in some limits (see the Settings section). We need another explanation of the convergence. It might generate the ballistic transport of the hard core by the local thermal activation to cause this result. This mechanism is consistent with the dissociation-induced recovery proposed in [43].

$\bar{\kappa}$ of c-FPU β shows the anomaly at $l = 0$ but the converging behavior at $l = 2, 4$ and we observe the transient anomaly at $l = 4$ where the exponent is the FH $\alpha \simeq 1/3$. First, the

---

[2]This is a prefetch but one cannot see the gradient increasing at the edges in this case, which is a characteristic feature of anomalous systems [49].
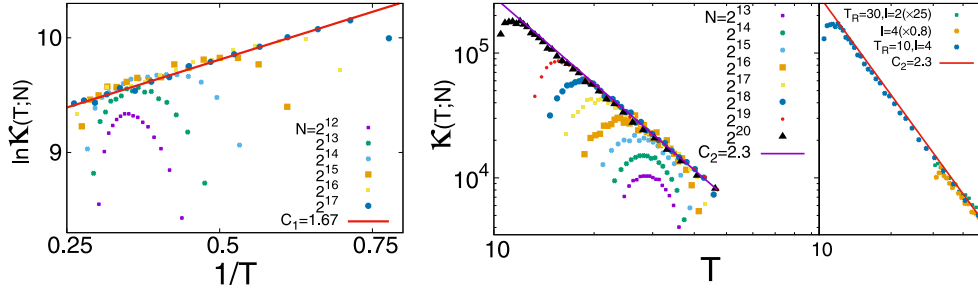
FIG. 3. Local heat conductivity (left: PR-6; center and right: c-FPU β). Parameters are $(T_L, T_R, d) = (4, 1, 3/4)$ for PR-6 and $(T_L, T_R, l) = (50, 10, 4)$ for c-FPU β in the center panel. The right panel shows the values of FPU β at the largest size of our observations with multiplication of normalization factors. They can be fitted with a unique curve approximately. One can observe the two different types of temperature dependence: the Arrhenius type connected with the thermally activated recovery in PR-6 and the non-Arrhenius type in c-FPU-β, suggesting another process from thermal activation.

result at $l = 0$ is consistent with the ordinary understanding of anomalous heat conduction [16,19]. The difference of the trend from the previous results at $l = 0$ with small sizes is caused by the difference of reservoirs and by the definitions of the temperature gradient. In our case, the number of the attached particles is slightly larger, so the boundary resistance is rather small, and the direct measurement of gradients reduces the effect of temperature gaps to the observable. Second, $\overline{\kappa}$ at $l = 2$ changes the N dependence completely from the case at $l = 0$ and shows the converging behavior throughout the observation. This is inconsistent with ordinary predictions [11], then we calculated $\overline{\kappa}$ until $N > 10^4$ but the results were the same. Here we introduce the power measured from the last two points as the indicator of convergence. The power is $\alpha \simeq 0.018$ at $l = 2$, almost 20 times smaller than the predicted exponents. The increase goes to be saturated. At the last, $l = 4$ is the delicate case. We got the transient exponent $\alpha \simeq 1/3$ in $10^2 \lesssim N \lesssim 10^4$, which is consistent with the FH theory, but $\overline{\kappa}$ shows another trend at large N. There is a plateau at larger sizes. We checked the power from the last two points and got 0.009. It is the convergence. The weak exponents in FPU $\alpha\beta$ at some parameters are already observed in [41], but the converging behavior like our case was not reported in their studies. We can see the transient exponent smaller than 0.1 in the $l = 2$ case, so it may correspond to their reports of such weak exponents. The difference would be caused by the temperature or by finite size effects. We chose the high temperature ($T \geqslant 10$), highly nonlinear, and $N > 10^4$, but their choice was low $T (\leqslant 0.1)$, weakly nonlinear, and $N < 10^4$. Actually, the long time tail is sensitive to the energy. The result in [45] showed the normal-anomalous crossover around $e \sim 0.1$ in FPU $\alpha\beta$ (at $\alpha = 0.1$) of the same unit with us. Repeatedly we note the high temperature of our system. It is also hard to suppose the possibility of dissociation because of the system property. This is directly checked by the following results of the temperature dependence in the local heat conductivity.

One can doubt whether our results are transient plateaus. The flattening before the FH scaling is actually reported in the previous research [42]. Our case of FPU β also has such a flattening at $l = 2, 4$ in $N \lesssim 10^3$. However, one can see the convergence which is after the FH scaling at $l = 4$. This is not included in their studies. Next we study the local heat conductivity to avoid the rash conclusion, although our results of bulk heat conductivity suggested the recovery

of the intensive property accompanying the increase of pressure.

3. Temperature dependence of intensive local heat conductivity

Figure 3 is the result of local heat conductivity κ and shows the two asymptotic master curves $\kappa(T; \infty)$ accompanying the recovery of normal heat conduction. Here we call the suggesting master curve $\kappa(T; \infty)$. Although the secured convergence of $\kappa(T; N) \to \kappa(T; \infty)$ in the thermodynamic limit is still controversial, these N-independent curves are the strong evidence of the recovery. Obvious N dependence of κ means the breakdown of our assumption that the local heat conductivity is described by the local (T, P), and one can see such N dependence only at small sizes. From the master curves, one can see the Arrhenius T dependence in PR-6 which corresponds to the thermal activation of dissociation [43] and the non-Arrhenius one in c-FPU-β, which corresponds to a different mechanism from thermal activation.

κ of PR-6 shows the recovery of the intensive property and the Arrhenius temperature dependence,

$$\kappa(T, \infty) \sim e^{C_1/T}. \tag{17}$$

The recovery began from the bulk. C_1 is estimated as $C_1 \simeq 1.67 \pm 0.04$ from our fitting. It is already reported that soft rod systems also show the Arrhenius type heat conductivity given by the GK formula [43], and they claimed the effective vacancy, dissociation should cause the normal heat conductivity. Such a mechanism would be also realized in this case. The local dissociation is naturally understood as the high energy property in this system (integrable hard core).

$\kappa(T; N)$ of compressed FPU β at $(l, T_R) = (4, 10)$ recovers the intensive property from the hotter side of the bulk and converges to the power-law curve,

$$\kappa(T; \infty) \sim T^{-C_2}. \tag{18}$$

C_2 is estimated as $C_2 \simeq 2.30 \pm 0.01$ from our fitting. We note the replacement of T_R ($30 \to 10$) is done to obtain the sufficiently wide temperature range. The result looks robust against the replacement. Figure 3 (right) shows the values of FPU β at the largest size of our observations [$(T_R, l) = (30, 2), (30, 4), (10, 4)$, corresponding size $N = 2^{15}, 2^{17}, 2^{20}$] with multiplication of normalization factors ($\times 25, 0.8, 1$ respectively). They can be roughly fitted with a unique curve. The
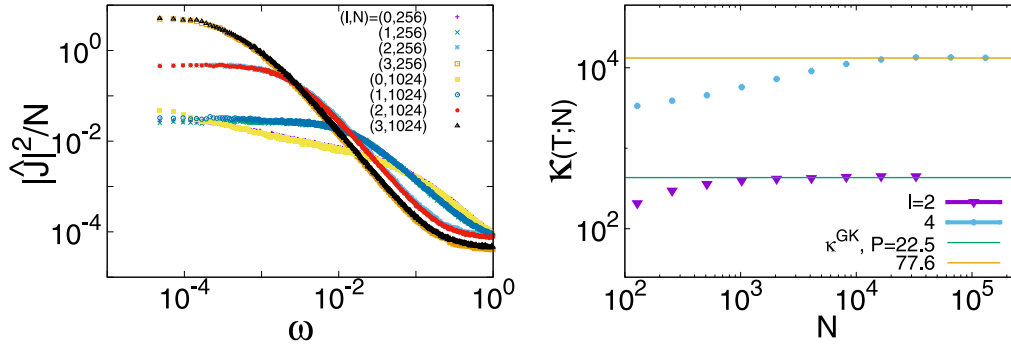
FIG. 4. Left: Normalized power spectra of the total energy currents $|\hat{J}(\omega)|^2/N$ of c-FPU β at $T = 30$ in $10^{-5} \lesssim \omega \lesssim 1$. Right: Comparison between the local heat conductivity at the averaged temperature $\bar{T}$ of steady heat conduction and the corresponding value given by the Green Kubo formula. One can see the anomalous scaling $|\hat{J}(\omega)|^2/N \sim \omega^{-\alpha}$ at small ω of $l = 0$, but Lorentzian $|\hat{J}(\omega)|^2/N \sim a/[1 + (b\omega)^2]$ recovers with l increasing ($l = 2,3$). There is no system size dependence at $l = 2,3$. The trends of (a,b) that (a,b) increase with l are consistent with Fig. 2. Pressure looks to suppress the long time tail. The comparison of heat conductivity (right) shows the consistent convergence of heat conductivity in highly compressed FPU β.

non-Arrhenius T dependence suggests another mechanism from some thermal activation. Taking into consideration the high T property of this system, the result of bulk heat conductivity and this non-Arrhenius T dependence, one can expect that this recovery of the intensive property may be understood with some continuum theory. We also observed the different exponent from the already reported $\kappa \sim T^{1/4}$ scaling of zero pressure FPU β [51]. The cause may be provided from the convergence of the heat conductivity or the pressure dependence of the heat conductivity because of the effect that the density fields of FPU β becomes spatially nonuniform to satisfy the constraint of uniform (P,J) conditions except $P = 0$. We also observed almost the same scaling at $l = 2$, then it may come from the normal-anomalous crossover. More accurate discussions on this change of the T dependence across the crossover need other experiments from ours. We first took the assumption that the global coupling is negligible. This assumption cannot be applied in anomalous heat conduction. Our interest is the difference of the temperature dependence from the already reported Arrhenius one and it was shown, so we do not go into the detailed discussion of this difference here.

B. Result of equilibrium simulation

It was suggested through the observations of steady heat conduction that there should be a thermally activated recovery of the heat conduction and that of continuums. Particularly, the latter case showed a striking negative example for ordinary fluctuating hydrodynamic predictions. Then we also study the convergence of heat conductivity through the observations of total energy current power spectra under the isolated equilibrium periodic boundary conditions to check our problematic result. Here we assume the equivalence of ensembles and change the boundary conditions from the isobaric isothermal $\langle \rangle_{T,P}^{\text{eq}}$ to the isothermal isodense $\langle \rangle_{T,l}^{\text{eq}}$. We studied its power spectra $|\hat{J}(\omega)|^2$, the Fourier components of the correlations $\langle \hat{J}(0)\hat{J}(t) \rangle_{T,l}^{\text{eq}}$, and their l dependence.

We beforehand discuss the validity of such equivalence. It is necessary to characterize the heat conductivity by a single value of temperature T that the temperature difference is suf-

ficiently small in the correlation length of the energy current, but such a length does not exist in the systems of anomalous heat conduction [24,28]. The quantitative correspondence of the heat conductivity in globally far from equilibrium with the correlation function in the isolated periodic boundary is actually a delicate problem [42,52]. Nevertheless, one can observe the long time tails of the currents under the isolated periodic boundary conditions and these scalings of the anomaly show the correspondence even with such changes of boundaries (see the $l = 0$ case of Fig. 4), furthermore, one can see the correspondence well because of the absence of boundary perturbations [17,34].

Figure 4 (left) shows normalized power spectra of total energy currents $|\hat{J}(\omega)|^2/N$ in compressed FPU β at $T = 30$. The anomalous scaling $|\hat{J}(\omega)|^2/N \sim \omega^{-\alpha}, \alpha = 1/3$ is observed in the $l = 0$ case of zero pressure. The strong exponent observed at high frequencies corresponds to the next FH exponent $4/3$. However, the $l = 1$ case shows no FH scaling at low frequencies although one can see the next FH $4/3$ tails at high frequencies. Then it asserts that the FH tail in low frequencies is suppressed by the compression. The scaling changes to the Lorentzian at highly compressed cases ($l = 2,3$) and one can see the clear suppression of the anomaly at low frequencies. The trend in the Lorentzian of the height and that of the time scale are consistent with our experiment of steady state heat conduction that they increase with compression. We checked the N convergence of the Lorentzian and the results at $N = 256,1024$ were the same. In the ordinary understanding, if the *ad hoc* cutoff of the anomaly $\omega > 2\pi c/N$ is valid also under this condition, the spectra at $l = 1,2,3$ should show the long time tails at the same area with the $l = 0$ case, except the improbable explosion of t_m with l increasing, because the sound velocity is only doubled through the l increasing ($l = 0 \to 3$ at $T = 30$). The result that there is only the $4/3$ exponent (no $1/3$) at $l = 1$ and the Lorentzian recovery at $l = 2,3$ suggests that the compression (pressure) should induce the suppression.

This result of equilibrium correlations should show the quantitative correspondence with our result of steady heat conduction if the convergence is not a fake. The Green Kubo formula requires that a variable given by the equilibrium

correlations $N^{-1} \int_0^\infty dt \langle \hat{J}(0)\hat{J}(t) \rangle_{T,P}^{\rm eq}$ and heat conductivity of the system $\kappa_*(T,P,N)$ take a same value, that is

$$\lim_{N \to \infty} \left(\frac{1}{N} \int_0^\infty dt \langle \hat{J}(0)\hat{J}(t) \rangle_{T,P}^{\rm eq} - \kappa_*(T,P,N) \right) = 0. \quad (19)$$

In general, we should include the other orders of the system and in such a case, one can translate (T,P) into the whole intensive variables conjugate with the conserved fields of the system except N. We can expect that FPU β should not have such additional orders because of the consistency between equilibrium correlations of FPU β and the prediction of fluctuating hydrodynamics for simple fluids [24]. Furthermore, if the system shows the normal heat conduction, the above relation becomes more tractable. First, energy currents in the systems of normal heat conduction have the finite correlation length, so heat conductivity is not modified under the change of boundaries if the change does not vary (T,P,N). It means

$$\frac{1}{N} \int_0^\infty dt \langle \hat{J}(0)\hat{J}(t) \rangle_{T,P}^{\rm eq} = \frac{1}{N} \int_0^\infty dt \langle \hat{J}(0)\hat{J}(t) \rangle_{T,l_*(T,P)}^{\rm eq}. \quad (20)$$

We defined $l_*(T,P)$ as the compression that gives the pressure P under the temperature T (and N). Also, in the system of normal heat conduction, heat conductivity is independent of the observational condition if (T,P) take the same values. It is another consequence of the locality guaranteed in the systems of normal heat conduction. Then, from the above relations, the question about the consistency between the variable given by the equilibrium correlations,

$$\kappa^{GK}(T,l,N) := \frac{1}{N} \int_0^\infty dt \langle \hat{J}(0)\hat{J}(t) \rangle_{T,l}^{\rm eq}, \quad (21)$$

and our local heat conductivity $\kappa(T,N)$ gives us the hint whether the numerical convergence captures the behavior in the thermodynamic limit. For this investigation, it is enough to check the relation

$$\lim_{N \to \infty} [\kappa^{GK}(T,l_*,N) - \kappa(T,N)] = 0. \quad (22)$$

We note the Green Kubo relation holds even at finite sizes if the observational condition and the size are the same, which can be proved with fluctuation theorem [53] (see Appendix A), but this is not guaranteed in different sizes or with different boundaries. So, this consistency becomes strong evidence of the convergence in the thermodynamic limit, though we cannot access the limit in the rigorous sense.

Figure 4 (right) shows the consistency between $\kappa^{GK}(T,l_*,N)$ of equilibrium simulations and $\kappa(T,N)$ of steady heat conduction at the averaged temperature of reservoirs $T = \bar{T}[:= (T_L + T_R)/2]$. As subtle but significant notation, l_* and l of nonequilibrium simulations of far from equilibrium conditions should not take the same value in general, because local compression of nonequilibrium simulations takes a different value from l. Homogeneity of pressure under the simulation is satisfied for the steady condition, so the choice of pressure avoids meaningless confusion. The values of pressure in nonequilibrium simulations are $P \simeq 22.5(l = 2), 77.6(l = 4)$ with Langevin reservoirs $(T_L = 30, T_R = 50, \bar{T} = 40, \gamma = 2, N = 2^{15}$, attached particle number $10 + 10)$ at the edges. The values of pressure were robust against the size in our case.

We measured κ^{GK} at the rather small sizes [$N = 1024(l = 2), 256(l = 4)$] on receiving the N independence as seen in the left panel of Fig. 4. Both cases of different compression $l = 2, 4$ show the quantitative correspondence with Green Kubo values at large sizes. The transient exponent at $l = 4$ is consistent with the corresponding bulk heat conductivity. This system shows the numerical consistency of two variables under the different conditions (of sizes and of boundaries). It strongly asserts the normal heat conduction which remains at the larger sizes.

C. Result of analysis

Our simulations showed two different types of temperature dependence on intensive heat conductivity. They suggest two mechanisms in the recovery of Fourier's law. The Arrhenius form connects to a thermally activated inhibitor and the non-Arrhenius one suggests a continuum mechanism different from the former. Here, we try to explain these processes phenomenologically.

1. Transition-state theory of thermally activated dissociation

Here we estimate the coefficient of the Arrhenius T dependence in PR-6 along the scenario of the thermally activated dissociation proposed in [43]. In PR-6, there is no FH scaling before the convergence and the temperature dependence is the Arrhenius form. This result suggests the possibility that some noncontinuum effect would suppress the anomaly. According to them, this convergence is caused by the effective vacancy (dissociation) formation. Now we assume it as an effective point defect and estimate the effective activation energy to compare with our numerical result.

If one can define the maximum energy state on each vacancy formation path, according to the transition-state theory, the vacancy formation ratio $P_* \sim \exp(-E_*/T)$ can be decided by the minimum of their energy cost [54], i.e., E_* is the energy difference between the maximum energy and the minimum energy on the path to generate a defect with the smallest energy cost. In this case, the path corresponds to the quasistatic path, then E_* corresponds to the minimum energy benefit to make a vacancy at the bulk. Concretely, as the minimum work to make a vacancy of the characteristic length d at the bulk including N particles, one can estimate E_* as

$$E_* \sim N \left\{ V \left(d \left(1 - \frac{1}{N} \right) \right) - V(d) \right\} - V(d) \quad (23)$$

$$\simeq -\frac{\partial V(d)}{\partial d} d - V(d). \quad (24)$$

Then, the minimum length which has a vacancy in average would be

$$N_* \sim P_*^{-1} \sim e^{E_*/T}. \quad (25)$$

Then, assuming the scaling $\kappa \sim N^\alpha$ is saturated at N_*, the temperature dependence of κ is given by

$$\kappa \sim N_*^\alpha \sim e^{\alpha E_*/T}. \quad (26)$$

We compare the estimation with the numerical value: $C_1 \simeq 1.7 \sim 2$. We derive the value: $C_1 \sim 2.341 \sim 2$ from the above discussion with $\alpha \simeq 1/2$ of the simulation. The mechanism

of the recovery caused by the thermally activated point defect gives an approximate picture to this convergence, even though the dissociation is not well defined in this system. One can take elastically colliding systems like in [43] as the model systems for more accurate treatments, where the dissociation is safely defined.

2. Fluctuating hydrodynamic description of the pressure-induced recovery

We investigate how the pressure fluctuation changes the observed transport coefficients here. Our numerical simulations suggest that there would be a pressure-induced mechanism of the recovery of Fourier's law in one-dimensional momentum-conserving systems. This non-Arrhenius temperature dependence is inconsistent with the scenario of thermally activated dissociation, so we should consider the recovery with some continuum theory. Here we consider the mechanism with the fluctuating hydrodynamics.

One-dimensional full fluctuating hydrodynamic equations describe the slow motion of the conserved quantities (: mass, momentum, and energy) and consist of the following equations of continuity, writing (ρ, v, e) as mass density, velocity, and energy density:

$$\partial_t \rho + \partial_x(\rho v) = 0,$$

$$\partial_t(\rho v) + \partial_x(\rho v^2 + \sigma) = 0, \sigma = P - \mu \partial_x v - s,$$

$$\partial_t e + \partial_x J = 0, J = ev + v\sigma - \kappa \partial_x T - g. \quad (27)$$

Here (P, T) express pressure and temperature and are the functions of mass density and internal energy density $(\rho, e - \rho v^2/2)$. (μ, κ) are bulk viscosity and heat conductivity. (s, g) are random stress and random heat current. The currents of momentum and those of energy include dissipation terms which consist of the deterministic part expressed as the linear irreversible process and the stochastic part satisfying fluctuation dissipation relation (FDR) [35]. (s, g) are described by the white noise as a consequence of the central limit theorem, and satisfy the following relations expressing the local FDR, using $\langle \rangle$ as the noise average:

$$\langle s(x,t)s(x',t')\rangle = 2\mu T \delta(x - x')\delta(t - t'),$$

$$\langle g(x,t)g(x',t')\rangle = 2\kappa T^2 \delta(x - x')\delta(t - t'),$$

$$\langle s(x,t)g(x',t')\rangle = 0. \quad (28)$$

In addition, the high wave number cutoff Λ is assumed because of the noncontinuum area of short wavelength.

We want to derive some simple model to study the effect of compressibility based on these equations here. We treat our equilibrium result as the observation of the anomaly suppression, then do not consider the nonequilibrium effects. Our treatment to discuss the convergence also neglects the nonlinear terms of dissipation terms, because they are irrelevant even in the inviscid scaling [15]. We restrict our attention in such a parameter range. We write $(\rho, u := \rho v, e)$ as mass density, momentum density, and energy density, and study the fluctuations $(\delta \rho, u, \delta e)$ from the base of a static equilibrium state $(\rho_0, 0, e_0)$. Their motion is described by the following equations, at the lowest order of nonlinearity

neglecting irrelevant dissipative nonlinear terms,

$$\partial_t \delta \rho + \partial_x u = 0,$$

$$\partial_t u + \frac{1}{\rho_0} \partial_x u^2$$

$$= -\left(\frac{\partial P}{\partial \rho}\right)_0 \partial_x \delta \rho - \left(\frac{\partial P}{\partial \rho}\right)_0 \partial_x \left(\delta e - \frac{u^2}{2\rho_0}\right)$$

$$+ \nu_0 \Delta u + \partial_x s_0 - \frac{1}{2} \partial_x \left[\left(\frac{\partial^2 P}{\partial \rho^2}\right)_0 (\delta \rho^2)\right]$$

$$+ 2\left(\frac{\partial^2 P}{\partial \rho \partial e}\right)_0 \delta \rho \delta e + \left(\frac{\partial^2 P}{\partial e^2}\right)_0 \delta e^2 \Bigg],$$

$$\partial_t \delta e + \frac{1}{\rho_0} \partial_x(u \delta e)$$

$$= -h_0 \partial_x u + \kappa_0 \left(\frac{\partial T}{\partial \rho}\right)_0 \Delta \delta \rho + \kappa_0 \left(\frac{\partial T}{\partial e}\right)_0 \Delta \delta e + \partial_x g_0$$

$$- \frac{e_0}{\rho_0} \partial_x \left(u \frac{\delta \rho}{\rho_0}\right) - \partial_x \left[u/\rho_0 \left(\left(\frac{\partial P}{\partial \rho}\right)_0 \delta \rho\right)\right.$$

$$\left. + \left(\frac{\partial P}{\partial \rho}\right)_0 \delta e\right)\Bigg]. \quad (29)$$

We defined $(\nu_0 := \mu_0/\rho_0, h_0 := (P_0 + e_0)/\rho_0)$ and 0 is the indicator of original equilibrium values. The derivation of the above equations is almost the same as in [15]. Spohn chose the particle distance as a conserved quantity instead of mass, but this is basically equivalent [55]. The nonlinear terms arise from pressure nonlinearity and Galilean invariance of fluids. Pressure nonlinearity is well studied in Spohn's papers. He assumed fluid equations in the particle currents (Lagrangian description) and no streaming terms appear in the description. Compared with pressure, streaming terms seem to have attracted less attention in spite of the famous mechanism of the anomaly induced by them [29]. Then we continue the analysis with the approximation of weak pressure fluctuations here to study the other origin of nonlinear effects. For further approximation, we treat the pressure fluctuations as the perturbations and neglect the corresponding nonlinear terms. We also neglect the nonlinear term including $(\delta \rho / \rho_0)$ taking into account the arbitrarily large lattice constant of lattice systems, then get the following equations:

$$\partial_t \delta \rho + \partial_x u = 0,$$

$$\partial_t u + \frac{1}{\rho_0} \partial_x u^2 = -Y_0 \partial_x \delta \rho - Z_0 \partial_x \delta e + \nu_0 \Delta u + \partial_x s_0,$$

$$\partial_t \delta e + \frac{1}{\rho_0} \partial_x u \delta e = -h_0 \partial_x u + D_0 \Delta \delta e + E_0 \Delta \delta \rho + \partial_x g_0. \quad (30)$$

Here we defined the coefficients $Y_0 := \left(\frac{\partial P}{\partial \rho}\right)_0, D_0 := \kappa_0 \left(\frac{\partial T}{\partial e}\right)_0,$ $Z_0 := \left(\frac{\partial P}{\partial \rho}\right)_0,$ and $E_0 := \kappa_0 \left(\frac{\partial T}{\partial \rho}\right)_0.$ D_0 is positive in general. h_0 can take the negative values, e.g., negative h_0 corresponds to some expanded states in FPU β. In the $Z_0 = 0$ case, corresponding to zero pressure in FPU β, Y_0 is positive because the sound velocity takes the real value. Particularly, $(Y_0, Z_0, h_0, E_0 \to 0)$ corresponds to the dynamics of the passive scalar on noisy Burgers fluids [56], and the divergence of observed transport coefficients (ν, D) obeys the inviscid

scaling [25,29]. Then, one can see this model as a minimal model to study the effect of compression.

The explicit calculation of renormalization into the observed transport coefficients on these equations clarifies how the pressure fluctuations affect the observed heat conductivity as a consequence of Galilean invariance. In particular, the $Z = 0$ (Z negligible) case is consistent with the *decoupling hypothesis* in [15], where the heat mode is passive to the sound modes, and we choose the parameter. Here, those waves are defined as the plane waves of perfect fluids. The propagation speed is zero in the heat mode and the sound speed in sound modes. The original decoupling hypothesis assumes the relation between plane waves only at the long wavelength. It means the asymptotic irrelevance of contribution from the heat to the sounds. The prediction based on the approximation is tested with good correspondence [24], so this hypothesis would capture the truth. We also emphasize that $Z = 0$ is the unique parameter satisfying the decoupling hypothesis except special sets of the coefficients. We put the MCT results under this parameter choice, which renormalizes the contribution of the higher wavelength fluctuations at once in the lowest order of nonlinearity [29]. The result of the heat diffusion coefficient takes the following value in the long wavelength and low frequency limit:

$$
\frac{D_R}{D_0} = 1 + \frac{T_0}{2\pi \rho_0 \sqrt{Y_0}\sqrt{D_0(D_0 + \nu_0)}} \frac{D_0 + 2\nu_0}{D_0 + \nu_0}
$$
$$
\times \left(2\arctan(W_0\Lambda) + \frac{(3D_0 + \nu_0)W_0\Lambda}{(D_0 + 2\nu_0)[1 + (W_0\Lambda)^2]} \right),
$$
$$
W_0 := \sqrt{\frac{D_0(D_0 + \nu_0)}{Y_0}}. \tag{31}
$$

This convergence is consistent with our numerical simulation. We note that the zero sound velocity limit ($Y_0 \to 0$) recovers the ordinary result of the D_R divergence ($D_R \to \infty$). Considering the difference between ours and the noisy Burgers solution ($Y_0 \to 0$ case), one can understand the convergence of the renormalized heat conductivity [$\kappa_R \simeq D_R/(\frac{\partial T}{\partial e})_0$] as the cutoff of the anomaly around the characteristic wave number $k_* := 2\sqrt{Y_0}/\nu_0$. This wave number is defined as the characteristic wave number of the momentum field Green function absorbing the density fluctuations, given by

$$
G_0(k,t) := \int \frac{d\omega e^{ikt+i\omega t}}{i\omega + \nu_0 k^2 - iY_0 k^2/\omega}, \tag{32}
$$

to show the effect of compressibility, i.e.,

$$
G_0(k,t) \simeq \begin{cases} e^{-\nu_0 k^2 t}, & k \gg k_* \\ e^{-(\nu_0 k^2/2)t}\cos\left(\frac{\nu_0 k_*|k|}{2}t\right), & k \ll k_*. \end{cases} \tag{33}
$$

Thus the compressibility would be intrinsic for this convergence. As other results, we derived the following:

$$
\frac{\nu_R}{\nu_0} = \infty, \tag{34}
$$

$$
\frac{h_R}{h_0} = 1 + \frac{(D_0 - E_0/h_0)T_0 \arctan(W_0\Lambda)}{2\pi\nu_0\rho_0\sqrt{Y_0}\sqrt{D_0(D_0 + \nu_0)}}, \tag{35}
$$

and $Y_R - Y_0, Z_R - Z_0, E_R - E_0 = 0$. $h_R \neq h_0$ is understood as the renormalization of the thermal fluctuations into the

energy. The value of the renormalized viscosity $\nu_R \to \infty$ asserts that the result of D_R is caused by some breakdown of the hyperscaling because two transport coefficients show the same scaling with sizes if the hyperscaling holds [29].

However, there are at least three problems for this interpretation. One is the unknown parameter ν_0. The above result of D_R asserts that the cutoff would be determined by the balance between viscosity and compressibility, but ν_0 is not observable. The second one is the correspondence of this result and the previous works which claim the divergence of heat conductivity in the inviscid limit. The third one is ν_R divergence. Some RG flow study can avoid the problems, but the RG study of those equations lacks brevity in spite of the unclear validity of our approximation.

The passive scalar limit, $Z_0 = h_0 = E_0 = 0$, extremely simplifies the problem, then we study the RG flow on this condition with believing some universality. This parameter simplification does not change our MCT results for the two transport coefficients D and ν. It means the results of our MCT analysis can be understood based on the following RG discussion. For further simplicity, we do not discuss the slightly messy flow of passive scalar here. Its flow does not affect the flow of the other conserved fields and should show the breakdown of the hyperscaling as the consistency with our MCT analysis (i.e., the value is absorbed into 0 under the flow). Then our starting point is

$$
\partial_t \delta\rho + \partial_x u = 0,
$$
$$
\partial_t u + \frac{1}{\rho_0}\partial_x u^2 = -Y_0\partial_x\delta\rho + \nu_0\Delta u + \partial_x s_0. \tag{36}
$$

These equations correspond to fluctuating hydrodynamic equations where pressure is temperature-independent and weakly fluctuates. $c_0 := \sqrt{Y_0}$ is the original sound velocity. One can do the same diagram calculation with the noisy Burgers case [29], then we briefly report the results. We introduce the formal nonlinear intensity λ and replace $1/\rho_0$ with $\lambda_0 := 1/\rho_0$. We write the noise intensity as Σ, $\Sigma_0 := 2\rho_0\nu_0 T_0$ to avoid the confusion of notation and define the coefficients $\bar{Y} := 4Y/(\nu\Lambda)^2, \bar{\lambda} := \lambda\sqrt{\Sigma/(\nu^3\Lambda)}$ for preparation.

The renormalization of the contribution from short wavelength $\Lambda > |k| > \Lambda e^{-l}, u^> := u\theta(|k| - \Lambda e^{-l})$ to long wavelength $|k| < e^{-l}, u^< := u - u^>$ and the rescaling along the scaling of u, $k' := e^l k$, $\omega' := e^{\int_0^l z(l')dl'}\omega$, $u^< =: \zeta u'$, $y(l) := \frac{d}{dl}\ln\zeta - (z + 1/2)$ shape the following RG flow:

$$
\frac{d\nu}{dl} = \nu\left(z - 2 + \frac{\bar{\lambda}^2}{2\pi}\right), \tag{37}
$$

$$
\frac{d\Sigma}{dl} = \Sigma\left(z - 2 - 2y + \frac{\bar{\lambda}^2}{2\pi}\frac{1}{\sqrt{1 - \bar{Y}^3}}\right), \tag{38}
$$

$$
\frac{d\lambda}{dl} = \lambda(-3/2 + z + y), \tag{39}
$$

$$
\frac{dY}{dl} = Y(-2 + 2z). \tag{40}
$$

ζ is chosen to make the same RG flow of (ν, Σ), and z is chosen as ν fixed at their initial values. The values are
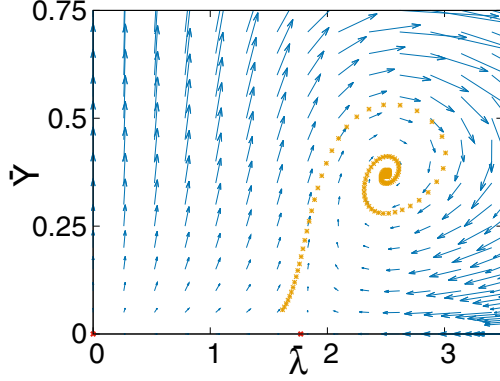
FIG. 5. The RG flow field (43) and (44) of approximated full fluctuating hydrodynamic equations in the passive scalar limit. There are four fixed points: $(\bar{\lambda}, \bar{Y}) = (0,0)$, $(0,\infty)$, $(\sqrt{\pi}, 0)$, $(\sqrt{2\pi}, 1 - 2^{-2/3})$. The latter two points are the well-known inviscid fixed point and the nontrivial ballistic fixed point. The linearly stable fixed point is the ballistic fixed point only. The inviscid fixed point is unstable except in $\bar{Y} = 0$. We marked the three fixed points taking finite values and show the typical flow in the same figure. $\bar{Y}$ slowly increases around the inviscid fixed point and the flow is accelerated after the detachment and wraps around the ballistic fixed point.

$$y = \frac{\bar{\lambda}^2}{4\pi}\left[\frac{1}{\sqrt{1 - \bar{Y}}^3} - 1\right], \tag{41}$$

$$z = 2 - \frac{\bar{\lambda}^2}{2\pi}. \tag{42}$$

Under the choice, the RG flow is reduced to

$$\frac{d\bar{Y}}{dl} = \bar{Y}\left(2 - \frac{\bar{\lambda}^2}{\pi}\right), \tag{43}$$

$$\frac{d\bar{\lambda}}{dl} = \bar{\lambda}\left[\frac{1}{2} - \frac{\bar{\lambda}^2}{4\pi}\left(3 - \frac{1}{\sqrt{1 - \bar{Y}}^3}\right)\right]. \tag{44}$$

We put the flow in Fig. 5. Now one can find four fixed points: the trivial Gaussian fixed point $(\bar{\lambda}, \bar{\lambda}, y, z) = (0,0,0,2)$, the well-known inviscid fixed point $(\bar{\lambda}, \bar{Y}, y, z) = (\sqrt{\pi}, 0, 0, 3/2)$, the $\bar{Y}$ divergent Gaussian fixed point $(\bar{\lambda}, \bar{Y}, y, z) = (0, \infty, 0, 2)$, and the other nontrivial fixed point $(\bar{\lambda}, \bar{Y}, y, z) = (\sqrt{2\pi}, 1 - 2^{-2/3}, 1/2, 1)$. Here we call it the *ballistic* fixed point because of its z value $z = 1$. Gaussian fixed points are unstable in one dimension as already pointed out [29], and the situation is the same in this analysis. It is noteworthy that only the ballistic fixed point is linearly stable. The $\bar{Y}$ divergent Gaussian fixed point is unstable in $\bar{\lambda} > 0$, so it would have no meaning because we started the analysis with $\bar{\lambda}_0 \neq 0$. The inviscid fixed point is unstable to the $\bar{Y}$ direction and stable only in $\bar{Y} = 0$. If the system at the point is perturbed to the $\bar{Y}$ direction, $\bar{Y}$ increases and the flow is absorbed to the ballistic fixed point. This result corresponds to the anomaly cutoff in our MCT analysis. We repeat the positivity of $\bar{Y}_0$ in this case.

With the above results, one can interpret the anomaly cutoff of the observed heat conductivity as some crossover between those two fixed points. The cutoff is determined by the characteristic wave number Λ_* where viscosity and compressibility are balanced. Λ_* is defined as the minimum

wave number satisfying the following relation:

$$\frac{2c}{\nu(\Lambda_*)\Lambda_*} = 1. \tag{45}$$

These quantities are observable. If the system obeys the inviscid scaling, one can roughly estimate ν as $\nu(k) \sim k^{-1/3}$ then the viscous fluids have such Λ_* because of $c > 0$. The corresponding system size $N_* := 2\pi/\Lambda_*$ is also given if Λ_* exists. Now, the scenario asserted from the results is as follows. At first, heat conductivity increases obeying the inviscid scaling in the small system sizes $N \ll N_*$, but the trend changes at $N \sim N_*$ and the heat conductivity shows the convergence at the larger system sizes $N \gg N_*$, i.e.,

$$\kappa \sim [\,\min[N, N_*]\,]^{1/3}. \tag{46}$$

The flow stagnates around the inviscid fixed point, then there can be a certain period to show the anomaly. The result is consistent with the result of c-FPU β at ($l = 4, T \gg 1$) where bulk heat conductivity increases with $\alpha \sim 1/3$ transiently and shows the tendency of saturation at larger system sizes. The result at $l = 2$ showing the rapid saturation can be interpreted as the case where initial $(\bar{\lambda}, \bar{Y})$ are near the ballistic fixed point.

The above scenario would be appropriately modified to include the obvious counterexample, the inviscid fixed point $(\bar{Y}, \lambda) = (0, \sqrt{\pi})$ in our analysis. This parameter $\bar{Y} = 0$ corresponds to the $l = 0$ case showing the agreement to the ordinary theories [11,15]. The stability of two nontrivial fixed points would be also changed by the effect of pressure nonlinearity. Even though, we expect that full analysis would keep the main ideas of this discussion, that the convergence our simulation captured would be connected to the crossover between two fixed points in the intermediate wavelength. According to our RG analysis, there can be a transition in the long wavelength limit of full fluctuating hydrodynamics.

IV. DISCUSSION

Here we discuss the correspondence between our results and previous works: the RG flow results (explicit calculations of noisy incompressible fluids, those of noisy Burgers fluids [29] and the scaling analysis [11]), MCT results of full FH (for the scaling of equilibrium correlators [15] and for steadily sheared systems [57]), numerical simulations, and the carbon-nanotube experiments [20].

Thermally activated dissociation and pressure fluctuations would cause the recovery of Fourier's law in one-dimensional momentum-conserving systems. The integrable systems at the dilute (high-energy) limit (e.g., PR-δ [41] and soft rod [43]) would be the models of the thermally activated recovery. The poly(quasi)stable interaction potential systems like the coupled rotator model would be also in this class for the same reason. The direct calculation of heat conductivity in the coupled rotator model with on-site potential predicts the Arrhenius T dependence [33]. With the same mechanism, the carbon nanotube may also show the saturation caused by thermally generated defects which is not avoidable in the real experiments [58]. The dissociation discussed here is not static and did not get the sufficient test. In addition, the relation between the dissociation class and nearly integrable systems which show the convergence (e.g., diatomic hard core with

small mass difference [46]) is still unclear. Further study is needed. Also, we note that one can see the long time tails of energy currents in diatomic PR-6 at the golden mass ratio. The reason would be the nonintegrability in its dilute limit (diatomic hard core). At the same time, the sum of momentum in each set of the same mass particles shows the long time tail, which means this observable is effectively conserved. The diatomic systems may need careful treatments [46,50]. The previous numerical simulation reporting the importance of the ballistic behavior in normal heat conduction [59] was criticized because of their zero-temperature simulations [60], but our following ballistic scaling observation is at the high temperature, where the system shows the anomaly at zero pressure. Potential asymmetry makes nonzero pressure, thus this ballistic-inviscid crossover on the RG flow may give some insight to the controversial systems of the convergence like FPU α,β and LJ [4,40–42,44,61]. For the real experiments, if our discussions are right, the dominance of these two effects is not clear, so it is also of interest to find the system showing the two mechanisms (corresponding to two temperature dependence). The multiparticle collision system [45] is intriguing. The recovery of Fourier's law in the thermodynamic limit should also still be discussed.

The continuum suppression of the anomaly is caused by the response to the pressure fluctuations in our analysis, and then compressibility can be an intrinsic factor. Our analysis considers the pressure fluctuations at the base of the linearized hydrodynamics and the wave number of saturation is decided with the sound velocity ($\sqrt{Y_0}$). In incompressible fluids, the pressure effect is the first order of nonlinearity [then $\mathcal{O}(l)$] and the response to the pressure becomes the second order [then $\mathcal{O}(l^2)$], so the (first derivative) RG flow of incompressible fluids [29] does not include this saturation. In the zero sound velocity limit, our result corresponds to the noisy Burgers result [25,29]. We repeat that our RG result demonstrated the instability of the inviscid fixed point to the assignment of compressibility. The property and the validity of our equations in the $d > 2$-dimensional cases, where the RG flow of noisy Burgers has an unstable fixed point [29], should be tested.

It may be constructive to derive the ballistic fixed point along the discussion deciding the anomalous exponent [11] here. First, we rescale time and space as $x = x'e^l$, $t = t'e^{zl}$, and assume the conserved fields we choose ($\rho, \mathbf{u}, e$) take the same scaling, ($\rho, \mathbf{u}, e$) $= \zeta(\rho', \mathbf{u}', e')$. Then, if the mass conservation law $\partial_t \rho + \nabla \mathbf{u} = 0$ is required to be invariant under the RG flow, t and x scale in the same way because of the required assumption. This is the desired exponent $z = 1$. This scaling discussion is in contrast to the discussion in [11] which required the same rescaling of the set ($\rho, \mathbf{v}, e$), where the scaling ($z = 3/2, d = 1$) is derived from the requirement of the same scaling of ($\rho, \mathbf{v}, e$), relevance of nonlinearity in the flow and the scaling invariance of the equal-time equilibrium fluctuations $\int dx^d(\rho^2, \mathbf{v}^2, e^2)$ under the flow (long range Gaussian property in their terms). In their discussions, the scaling dimension of the three variables is $-d/2$ and it corresponds to $-(d/2 + z)$ if the variables are treated as densities of the time directions (as a roughly sketched example, $\rho \to \rho \Delta t$) as described in [29]. The second assumption is satisfied in $d < 2$ dimension. The

last assumption can be understood as the extensive property of the fluctuations. Then, in other words, one can get the ballistic fixed point if one replaces the extensive fluctuations of ($\rho, \mathbf{v}, e$) with those of ($\rho, \mathbf{u}, e$) in their discussion. We also note that the scaling exponent $z = 1$ is *independent of the dimension* in this discussion. We do not know the meaning. Our scaling discussion expanded here is of heuristics and apparently has no use for the stability, but our example of the RG flow showed the possibility that compressibility should make the flow around the inviscid fixed point unstable.

In addition, the MCT analysis under sheared conditions (nonequilibrium steady states) already reported the tail strengthening, corresponding to the normal transport [57]. This may work as an analogy of the possibility that the nonequilibrium effect causes the convergence. They reported that the tail exponent changed at the characteristic wave number of the shear and that the strengthened exponent of the long wavelength corresponded to the normal transport. We did not discuss such a possibility here, but it is not hard to suppose that the nonequilibrium condition (isobaric but varying temperature) may affect the heat conduction because of the global coupling as in the GK formula [52].

At last, we go back to the most detailed MCT analysis of equilibrium correlations in one-dimensional full FH [15] for the discussion of the correspondence. We mention the difference that our analysis and Spohn's analysis are based on different equations. He started the analysis from the equations of continuity of conserved quantities (volume, momentum, and total energy), studied the effect of pressure nonlinearity with MCT and with some approximations, and got the scalings of the autocorrelation functions for the three plane waves of the linearized perfect fluids (one heat mode and two sound modes). His analysis is based on the linearized hydrodynamics added pressure nonlinearity. In his analysis, the anomaly is directly connected with the heat-heat mode correlator which becomes to the symmetric Levy distribution in sound cones propagating at the sound speed. His prediction is already tested in some anomalous systems with good agreements, but some deviation was also reported [24]. He used some approximations, however he also claimed the possibility that his result remains without his approximations in his equations. His claim looks based on the mirror symmetry of sound cones and nonlinear terms of currents. Then the difference with us may come from the starting point equations. Spohn's equations do not include streaming terms because of the derivative along the constituent particles [55], then the nonlinear currents are mirror-symmetric because the pressure depends only on mass and on internal energy. However, our equations include streaming terms and the nonlinear current ($u\delta e$) is mirror antisymmetric. Our result may assert the significance of this difference. One can have some questions to the validity of our D_R convergence, so to get the credit, we also note that the result of D_R (31) is also the exact solution of the passive scalar diffusion coefficient in the fluids neglecting their temperature dependence of pressure. As another derivation, one can easily get the same diagram of (30) with the same procedure of [62]. Then our result has the universality based on the ballistic fixed point to some extent.

To clarify the difference, the test of current fluctuations would be sufficient. His concrete prediction is as follows. First, he decomposed the conserved quantities $\mathbf{Q}_n =^T [\Delta x_n := x_n - x_{n-1}, p_n, \tilde{e}_n := V(\Delta x_n) + p_n^2/(2m)]$ into the three plane waves of the linearized perfect fluids $\tilde{\mathbf{Q}}_n$. If one obtains the linearized equations of perfect fluids $(\partial_t + \partial_x A)\mathbf{Q} = 0$ and the covariance matrix C s.t. $C_{mn} := \langle Q_m(x,t) : Q_n(y,s)\rangle_{T,P}^{\text{eq}}/[\delta(x - y)\delta(t - s)]$, one can define the linear transformation matrix R satisfying the conditions $RAR^{-1} = \text{diag}(-c, 0, c), RCR^T = \text{diag}(1, 1, 1)$ and derive $\tilde{\mathbf{Q}} := R\mathbf{Q}$. We used $\langle : \rangle_{T,P}^{\text{eq}}$ as $\langle f : g\rangle_{T,P}^{\text{eq}} := \langle fg\rangle_{T,P}^{\text{eq}} - \langle f\rangle_{T,P}^{\text{eq}}\langle g\rangle_{T,P}^{\text{eq}}$. One can decide R uniquely except the trivial arbitrariness ± 1. One of the sets takes the following matrix. See [55] for details. Here we abbreviate the time and the position for discussing the correlations of equal time and equal place. Shortening $\langle\rangle_{T,P}^{\text{eq}}$ to $\langle\rangle$, Δx_n to x, and $V(\Delta x_n)$ to V, and defining

$$\tilde{\Gamma}^{-1} := T^{-1}(\langle x : x\rangle\langle V : V\rangle - \langle x : V\rangle^2) + \frac{T}{2}\langle x : x\rangle \quad (47)$$

and

$$c := \tilde{\Gamma}\left(\langle(V + Px) : (V + Px)\rangle + \frac{T^2}{2}\right)$$

$$\tilde{Z}_1 := \sqrt{2T}c$$

$$\tilde{\kappa} := \sqrt{2T\tilde{\Gamma}}$$

$$\partial_l P := -\tilde{\Gamma}\left(\langle V : (V + Px)\rangle + \frac{T^2}{2}\right)$$

$$\partial_e P := \tilde{\Gamma}\langle x : (V + Px)\rangle, \quad (48)$$

we can define R as

$$R := \tilde{Z}_1^{-1}\begin{pmatrix} \partial_l P & -c & \partial_e P \\ \tilde{\kappa}P & 0 & \tilde{\kappa} \\ \partial_l P & c & \partial_e P \end{pmatrix}. \quad (49)$$

These values are easily calculated with the numerical integration of the corresponding canonical values. And then he derived the analytic formulas of $\tilde{\mathbf{Q}}$ autocorrelators [15]. One of the heat modes becomes symmetric Levy, and ones of the sound modes become the sound speed propagating KPZ.

Here we report the deviation with l increasing in c-FPU β, which looks like the asymptotic form with respect to t increasing. We set the data of the heat-heat correlator ($\Delta t = 0.005$, $T = 1$) in Fig. 6. We abbreviate the heat-mode autocorrelator S_h as S here. We only note about the sound modes that inclined sound-sound correlators already reported in [15] are also observed. The symmetric Levy distribution of the heat-heat correlator in the sound cones $S(x,t) \simeq t^{-2/3} f_I(x/t^{2/3})$ are observed at $l = 0$ [24], however, the phase difference of the sound cones looks tripled at $l = 0.5$. The deviation is consistent with our other results and also with the previous reports [24]. The height scaling looks to change at the same time. The observations of $S(0,t)$ show the change of the height scaling from $z = 3/2$ to $z = 1$. Furthermore, the heat-mode autocorrelator grows up around cones with the decreasing center top at $l = 1, 2$. The top is almost negligible at $l = 2$. We also note the bumps around the cones are scaled by x/t, which is just the ballistic scaling $z = 1$. This exponent change and growing bumps mean the scaling crossover from

the inviscid scaling $S(x,t) \simeq t^{-2/3} f_I(x/t^{2/3})$ to the ballistic scaling $S(x,t) \simeq t^{-1} f_B(x/t)$. The sound-heat correlations or the correlation overlaps [24] may affect the result. If the anomaly remains in his equations [15], this difference may come from streaming terms. We could not observe the cutoff of the scaling to provide the convergence, although the crossover is observed. It is difficult to observe the anomaly cutoff like $S(x,t) \simeq e^{-t/\tau} t^{-1} f_B(x/t)$ at the long time scale as already pointed out in [38] and we do not know what the possible cutoff looks like. We may need the extensive tests of the universality in one dimensional momentum-conserving systems.

V. CONCLUSION

Our numerical experiments of steady heat conduction suggested some possible origins of normal heat conduction in one-dimensional momentum-conserving systems. The recovery had been explained by the thermally activated dissociation. However, compressed FPU β under the strong compression and of high energy ($l = 2, 4, T \gg 1$) showed the recovery of Fourier's law with the non-Arrhenius T dependence of heat conductivity. It suggested the existence of the class of normal heat conduction, the origin of which is explained by some macroscopic continuum theory in one-dimensional momentum-conserving systems. There would be at least two mechanisms of normal heat conduction. The vanishing long time tails of total energy currents suggested some relation between the non-Arrhenius type recovery and the pressure. Then we tried to explain the two mechanisms with corresponding phenomenologies. First, for the case of the Arrhenius T dependence, we studied the coefficient with the transition-state theory following the scenario reported in [43] that the convergence is caused by the thermal activation of dissociation and got quantitative agreement with our numerical simulations of PR-6 in a certain extent. Second, for the case of the non-Arrhenius T dependence, we executed the MCT analysis based on full FH equations of a specific limit and got the suggestion that the pressure fluctuations suppressed the anomaly. This was consistent with our numerical result of compressed FPU β. The RG flow of further approximated equations asserted the connection between this result and the ballistic fixed point, another nontrivial fixed point from the inviscid fixed point. The fixed point was induced by the compressibility in our RG analysis. Discussing the correspondence with the previous accurate theory of equilibrium correlators [15], we found the possibility of the inviscid-ballistic crossover of the heat mode autocorrelator. Further investigation is needed to examine the possibility of normal heat conduction in one-dimensional momentum-conserving systems.
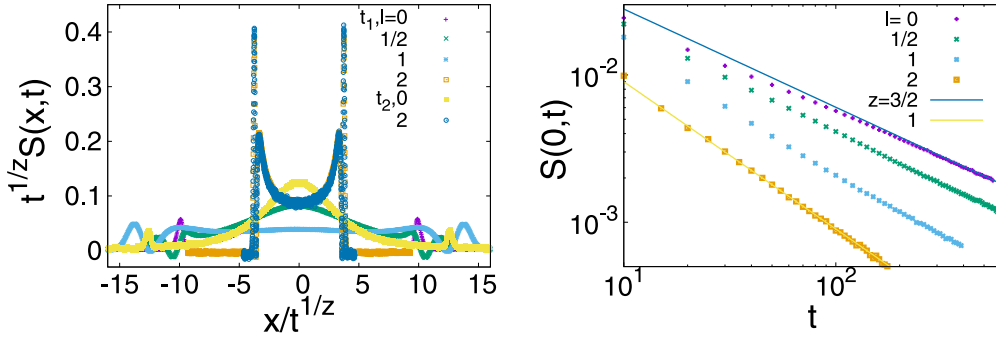
FIG. 6. Left: The equilibrium autocorrelation of the heat mode in c-FPU β at $T = 1$, $t = t_n \sim 400n/c$, $N = 2048$. Right: $S(0,t)$ in $t \leqslant t_2$. z values of the left panel are chosen as $z = 3/2$ at $l \neq 2$ and $z = 1$ at $l = 2$. One can see the symmetric Levy in sound cones at $l = 0$ and the growing bumps around the cones at $l \neq 0$. $S(x,t)$ shows the ballistic scaling at $l = 2$. The width scaling is the inviscid one $x/t^{2/3}$ at $l = 0$ and the ballistic one x/t at $l = 2$. $S(0,t)$ shows the clear crossover.

APPENDIX A: DERIVATION OF THE GREEN KUBO FORMULA

We derive the Green Kubo formula of the normal heat conduction here in two ways. One of them (A22) is the expansion from the globally equilibrium conditions and the other (A35) is the expansion from the locally equilibrium conditions. In the far from equilibrium conditions, one cannot use the former, but can use the latter.

1. Setting

Let us consider a system that connects to two stochastic reservoirs at the edges. Each reservoir has its connecting area and satisfies the local detailed balance condition. We assume the time-reversal symmetry of the system Hamiltonian and the nearest-neighbor interaction ("short range" interaction). We further assume the unique steady state ensemble P^{st} independent of the initial conditions. Here we consider the macroscopic variables along the particle index, but can translate it to that along the field coordinate $[A_i \to A(x) = \sum_i A_i \delta(x - x_i)]$. Under that translation, the choice of the variable $r_i(:= x_{i+1} - x_i)$ in the expansion from the local equilibriums would be translated into that of the mass density $\rho(x) = \sum_i m_i \delta(x - x_i)$. Also, one can extend this discussion to the case having additional order parameters.

We describe the fundamental relation to derive the formula as the preparation. We note Γ as the phase space coordinate and $\mathcal{H}$ as the system Hamiltonian. h_i is the ith particle energy density, $j_{i+1,i}$ is the corresponding energy current, and r_i is the ith particle compression here. $\beta_\pm(\beta_+ > \beta_-)$ is the temperature of the reservoir $\pm$. Energy conservation law can be written as

$$\partial_t h_i + j_{i+1,i} - j_{i,i-1} = \sum_\pm \dot{Q}_i^\pm \chi[i \in D_\pm], \quad \text{(A1)}$$

$$\chi[A] = \begin{cases} 1 & A: \text{true} \\ 0 & A: \text{false}. \end{cases} \quad \text{(A2)}$$

$D_\pm$ is the connecting area of the reservoir $\pm$ ($|D_\pm| \ll N$, N: system size) and $\dot{Q}_i^\pm$ is the energy from the reservoir $\pm$ to the ith particle per time. By the local detailed balance condition, the path probability on the path $\hat{\Gamma}$ within the time $t \in [0,\tau]$

and that on the time-reversal path $\hat{\Gamma}^\dagger$ satisfy the relation

$$\frac{P(\hat{\Gamma}|\Gamma_0)}{P(\hat{\Gamma}^\dagger|\Gamma_\tau^*)} = e^{-\beta_\pm Q_\tau^\pm}. \quad \text{(A3)}$$

Here, $Q_\tau^\pm$ is defined as $Q_\tau^\pm := \int_0^\tau \sum_{i \in D_\pm} \dot{Q}_i^\pm$, Γ_0 is the initial state of $\hat{\Gamma}$, and Γ_τ is the end state of $\hat{\Gamma}$. $*$ is the index that expresses the time-reversal quantity B^* of the instantaneous variable $B(\Gamma)$. $P(\hat{\Gamma}|\Gamma)$ is the conditional probability of the path under this thermostat condition.

It is convenient for later discussions to introduce McLennan ensembles (A15) [63,64]. First, we note that fluctuation theorem (A8) holds for path-dependent variables $\mathcal{A}(\hat{\Gamma})$ because of the existence of the local detailed balance (A3). Now we use $\langle \rangle$ as the average of the stochastic reservoir forces. Defining

$$\Sigma(\hat{\Gamma}) := \beta_\pm Q_\tau^\pm + \ln \frac{P^{\text{ref}}(\Gamma_0)}{P^{\text{ref}}(\Gamma_\tau^*)} \quad \text{(A4)}$$

and using $\dagger$ as the indicator of the time reversals of the path-dependent variables $[\mathcal{A}^\dagger(\hat{\Gamma}) = \mathcal{A}(\hat{\Gamma}^\dagger)]$, one can get

$$\langle \mathcal{A}(\hat{\Gamma}) \rangle := \int d\hat{\Gamma} \, P(\hat{\Gamma}|\Gamma_0) P^{\text{ref}}(\Gamma_0) \mathcal{A}(\hat{\Gamma}) \quad \text{(A5)}$$

$$= \int d\hat{\Gamma}^\dagger P(\hat{\Gamma}^\dagger|\Gamma_\tau^*) P^{\text{ref}}(\Gamma_\tau^*) \mathcal{A}(\hat{\Gamma})$$

$$\times \exp\left(\beta_\pm Q_\tau^\pm + \ln \frac{P^{\text{ref}}(\Gamma_0)}{P^{\text{ref}}(\Gamma_\tau^*)}\right) \quad \text{(A6)}$$

$$= \int d\hat{\Gamma} \, P(\hat{\Gamma}|\Gamma_0) P^{\text{ref}}(\Gamma_0) e^{\Sigma^\dagger(\hat{\Gamma})} \mathcal{A}^\dagger(\hat{\Gamma}). \quad \text{(A7)}$$

That is

$$\langle \mathcal{A} \rangle = \langle \mathcal{A}^\dagger e^{\Sigma^\dagger} \rangle. \quad \text{(A8)}$$

Second, we consider the time evolution of an ensemble P_τ that started from a reference ensemble P^{ref}. We choose $\mathcal{A} = \delta(\Gamma' - \Gamma_\tau)$ in the above fluctuation theorem, and get

$$P_\tau(\Gamma') = \langle \delta(\Gamma' - \Gamma_\tau) \rangle = \langle \delta(\Gamma' - \Gamma_0^*) e^{\Sigma^\dagger} \rangle \quad \text{(A9)}$$

$$= P^{\text{ref}}[(\Gamma')^*]$$

$$\times \int d\hat{\Gamma} \, P(\hat{\Gamma}|\Gamma_0) e^{\Sigma^\dagger(\hat{\Gamma})} \delta[\Gamma_0 - (\Gamma')^*]. \quad \text{(A10)}$$

We take the limit $\tau \to \infty$, and the steady distribution is expressed as

$$P^{st}(\Gamma) = P^{\text{ref}}(\Gamma^*)$$
$$\times \lim_{\tau \to \infty} \int d\hat{\Gamma}\, P(\hat{\Gamma}|\Gamma_0) e^{\Sigma^\dagger(\hat{\Gamma})} \delta(\Gamma_0 - \Gamma^*). \quad \text{(A11)}$$

We use $\langle\rangle^{st}$ to express the steady state average. This expression is transformed into another form for the instantaneous variables $B(\Gamma)$. Using the relation $d\Gamma = d\Gamma^*$, one can get the tractable form

$$\langle B \rangle^{st} = \int d\Gamma^* B^*(\Gamma^*)(P^{st})^*(\Gamma^*) \quad \text{(A12)}$$

$$= \int d\Gamma\, B^*(\Gamma)(P^{st})^*(\Gamma) \quad \text{(A13)}$$

$$= \lim_{\tau \to \infty} \int d\hat{\Gamma}\, B^*(\Gamma) P^{\text{ref}}(\Gamma) P(\hat{\Gamma}|\Gamma) e^{\Sigma^\dagger(\hat{\Gamma})}, \quad \text{(A14)}$$

namely

$$\langle B \rangle^{st} = \lim_{\tau \to \infty} \langle B^* e^{\Sigma^\dagger} \rangle^{\text{ref}}. \quad \text{(A15)}$$

We expressed the reference ensemble average as $\langle\rangle^{\text{ref}}$.

2. Derivation

a. Derivation 1: Expansions from globally equilibrium conditions

We consider the expansion from the static globally equilibrium state

$$(\langle r_i \rangle^{st}, \langle p_i \rangle^{st}, \langle h_i \rangle^{st}) = (l, 0, e). \quad \text{(A16)}$$

Corresponding intensive variables are

$$(\beta P, \beta V, \beta) = (\bar{\beta} P_0, 0, \beta), \quad \bar{\beta} = \frac{\beta_+ + \beta_-}{2}. \quad \text{(A17)}$$

P is the pressure and V is the averaged velocity. Now we choose

$$P^{\text{ref}} = P_{\bar{\beta}}^{\text{can}} := e^{-\bar{\beta}\mathcal{H}}/Z \quad \text{(A18)}$$

as the reference ensemble. It means the choice of (T, l). We use $\langle\rangle_{\bar{\beta}}^{\text{can}}$ to express the average by the ensemble $P_{\bar{\beta}}^{\text{can}}$. Entropy production Σ takes the form

$$\Sigma = -\beta_\pm Q_\tau^\pm + \bar{\beta}[\mathcal{H}(\Gamma_\tau^*) - \mathcal{H}(\Gamma)] = \Delta\beta Q. \quad \text{(A19)}$$

We used the time-reversal symmetry of the Hamiltonian $\mathcal{H}(\Gamma_\tau^*) = \mathcal{H}(\Gamma_\tau)$ and defined $\Delta\beta := \beta_+ - \beta_-, Q := (Q_- - Q_+)/2$. Corresponding time reversals are $\Sigma^\dagger = -\Delta\beta Q, \dot{Q}^* = -\dot{Q}$. The energy conservation law of the systems at the steady states requires $\sum_\pm \langle \dot{Q}^\pm \rangle^{st} = 0$. Also, the energy balance at the bulk $(n \in D_\pm)$ yields the relation

$$|\langle J \rangle^{st}| := |\langle j_{n+1,n} \rangle^{st}| = \langle \dot{Q} \rangle^{st} \quad \text{(A20)}$$

$$= \lim_{\tau \to \infty} \langle -\dot{Q} e^{-\Delta\beta Q} \rangle_{\bar{\beta}}^{\text{can}} \quad \text{(A21)}$$

$$= \Delta\beta \int_0^\infty dt \langle \dot{Q}(0)\dot{Q}(t) \rangle_{\bar{\beta}}^{\text{can}} + \mathcal{O}[(\Delta\beta)^2]. \quad \text{(A22)}$$

The sign of J is minus if the reservoir $+$ is at the left and plus if it is at the right. The error from the relation can be large if $\Delta\beta$ is comparable with $\bar{\beta}$ and not negligible in that case.

b. Derivation 2: Expansions from locally equilibrium conditions

One can know the steady state value of the energy and the compression through the careful observation even if their values spatially change, and we consider the expansion from the static locally equilibrium conditions

$$(\langle r_i \rangle^{st}, \langle p_i \rangle^{st}, \langle h_i \rangle^{st}) = (l_i, 0, e_i). \quad \text{(A23)}$$

Spatial homogeneity of pressure is needed to keep the zero value of the momenta, then corresponding intensive variables are

$$((\beta P)_i, (\beta V)_i, \beta_i) = (\beta_i P, 0, \beta_i). \quad \text{(A24)}$$

Now we suppose l_i and e_i are slowly varying quantities in space scaled with the correlation length of microscopic variables (particularly $j_{i+1,i}, v_i := p_i/m_i$). Also, we suppose the temperature gaps at the edges are negligible. If the system shows the normal heat conduction, one can realize them with sufficiently large (but finite) system sizes N. Under the condition, one can expand the contribution from the entropy production Σ around the local equilibriums. So we take the isobaric local equilibrium ensemble as the reference ensemble,

$$P^{\text{ref}} = P_{\{\beta_i\}_i, P}^{lc} := e^{-\beta_i h_i - [(\beta_{i+1} + \beta_i)/2]P r_i}/Z. \quad \text{(A25)}$$

It means the choice of $(\{T_i\}_i, P)$. β_i is chosen as the parameter satisfying the relation

$$i \bar{\in} D_\pm, \langle h_i \rangle_{\{\beta_i\}_i, P}^{lc} = \langle h_i \rangle^{st}; \quad i \in D_\pm, \beta_i = \beta_\pm. \quad \text{(A26)}$$

We use $\langle\rangle_{(\{\beta_i\}_i, P)}^{lc}$ to express the average by the ensemble $P_{\{\beta_i\}_i, P}^{lc}$. Entropy production takes the value

$$\Sigma = -\beta_\pm Q_\tau^\pm + \beta_i[h_i(\Gamma_\tau^*) - h_i(\Gamma)]$$
$$+ \frac{\beta_{i+1} + \beta_i}{2} P[r_i(\Gamma_\tau^*) - r_i(\Gamma)] \quad \text{(A27)}$$

$$= -\int_0^\tau dt \left[\beta_i(j_{i+1,i} - j_{i,i-1}) \right.$$
$$\left. - \frac{\beta_{i+1} + \beta_i}{2} P(v_{i+1} - v_i) \right] \quad \text{(A28)}$$

$$= \int_0^\tau dt \left[(\beta_{i+1} - \beta_i)j_{i+1,i} - \frac{\beta_{i+1} - \beta_{i-1}}{2} P v_i \right]. \quad \text{(A29)}$$

The time reversals are $\Sigma^\dagger = -\Sigma, j_{i+1,i}^* = -j_{i+1,i}$. Then the averaged value of the current at the bulk $n \sim N/2$ can be estimated as

$$\langle J \rangle^{st} := \langle j_{n+1,n} \rangle^{st} \quad \text{(A30)}$$

$$= \lim_{\tau \to \infty} \langle -j_{n+1,n}$$
$$\times e^{-\int_0^\tau dt\{(\beta_{i+1} - \beta_i)j_{i+1,i} - [(\beta_{i+1} - \beta_{i-1})/2]P v_i\}} \rangle_{(\{\beta_i\}_i, P)}^{lc} \quad \text{(A31)}$$

$$= \left\langle j_{n+1,n}(0) \int_0^\infty dt \left[(\beta_{i+1} - \beta_i)j_{i+1,i} \right.\right.$$
$$\left.\left. - \frac{\beta_{i+1} - \beta_{i-1}}{2} P v_i \right] \right\rangle_{(\{\beta_i\}_i, P)}^{lc} + \mathcal{O}[(d\partial_n\beta)^2]. \quad \text{(A32)}$$

d is the largest correlation length of the currents. $\langle j_{n+1,n} \rangle_{(\{\beta_i\}_i, P)}^{lc} = \langle j_{n+1,n}^* \rangle_{(\{\beta_i\}_i, P)}^{lc} = 0$ follows the time-reversal symmetry of the chosen ensemble reflecting

$\mathcal{H}^* = \mathcal{H}$. This relation corresponds to that derived by Casati and Prosen [52] under the chaotic pictures. However, the estimated error under the anomalous heat conduction is different from the above. Under the condition, the estimated error was $\mathcal{O}[(N\partial_n\beta)^2] = \mathcal{O}[(\Delta\beta)^2]$ because there were no scale separations anymore and the correlation length grows to the system size ($d \sim N$). The situation of the system of normal heat conduction is in sharp contrast to it. In the systems of normal heat conduction, this modified error estimation $\mathcal{O}[(d\partial_n\beta)^2]$ assures us the safety to use the relation even under the far from equilibrium conditions ($\Delta\beta \sim \bar{\beta}$). Our interest is in the Green Kubo formula on the systems of normal heat conduction, so the average of the right hand side can be estimated under the equilibrium condition with further expansions. Writing the ensemble average by the isobaric canonical $P^{\text{can}}_{\beta,P} := \exp[-\beta(\mathcal{H} + P\sum_i r_i)]/Z$ as $\langle\rangle^{\text{can}}_{(\beta,P)}$, we get the estimation

$$\langle J\rangle^{st} = (\beta_{n+1} - \beta_n)$$
$$\times \left\langle j_{n+1,n}(0)\int_0^\infty dt \sum_i [j_{i+1,i} - Pv_i]\right\rangle^{\text{can}}_{(\beta_n,P)}$$
$$+ \mathcal{O}((d\partial_n\beta)^2, d^2\partial_n^2\beta). \quad (A33)$$

We set a rule that we do not take the summation on the index n (though we have taken the summation on the index i). This relation is valid for each gradient $\beta_{n+1,n}(n \sim N/2)$, i.e., β_n dependence of the averaged current correlations corresponds to the temperature dependence of the heat conductivity ($\times\beta^{-2}$) in the isobaric cases. Also, at the middle of the system $n \sim N/2$, the forces from the reservoirs within the correlation time τ_c does not affect the dynamics of the particles far from the edges within the time and the contribution of the past forces from the reservoirs are used only for the setting of the initial condition; then one can estimate the average with static isolated-periodic boundary. This translation is done by the change of the conditional probability $P(\hat{\Gamma}|\Gamma) \to \delta[\hat{\Gamma}(\Gamma) - \hat{\Gamma}]$ [where $\hat{\Gamma}(\Gamma)$ is the solution of the equation of motion determined by the system Hamiltonian with the initial condition Γ], and we note it as $\langle\rangle^{\text{can}-IP}_{(\beta,P)}$. Then it can be reduced to

$$\langle J\rangle^{st} = (\beta_{n+1} - \beta_n)$$
$$\times \left\langle j_{n+1,n}(0)\int_0^\infty dt \sum_i [j_{i+1,i} - Pv_i]\right\rangle^{\text{can}-IP}_{(\beta_n,P)}$$
$$+ \mathcal{O}\left((d\partial_n\beta)^2, d^2\partial_n^2\beta, d\partial_n\beta\frac{c\tau_c}{N}\right). \quad (A34)$$

We repeat the no summation on the index n. The propagation speed of the effect is constrained by the sound speed c, so the error accompanying this translation is estimated as $\mathcal{O}(d\partial_n\beta \cdot c\tau_c/N)$. In the monatomic case, the second term vanishes because of the momentum conservation $\sum_i p_i = 0$, then

$$\langle J\rangle^{st} = (\beta_{n+1} - \beta_n)\frac{1}{N}\int_0^\infty dt\langle\hat{J}(0)\hat{J}(t)\rangle^{\text{can}-IP}_{(\beta_n,P)}$$
$$+ \mathcal{O}\left((d\partial_n\beta)^2, d^2\partial_n^2\beta, d\partial_n\beta\frac{c\tau_c}{N}\right). \quad (A35)$$

This is the desired relation. Here we defined $\hat{J} := \sum_i j_{i+1,i}$. Clearly, it can be used even if $\Delta\beta$ is comparable with $\bar{\beta}$. The perturbation is roughly estimated as $(\Delta\beta d)/(\bar{\beta}N)$. Smallness of the perturbation comes from the scale separation $d/N \ll 1$. The reverse transformation of the boundary $\langle\rangle^{\text{can}-IP} \to \langle\rangle^{\text{can}}$ and the change of the choice of the macroscopic variable $P \to l(T,P)$ recovers the ordinary Green Kubo formula as already discussed in the paper.

3. Remarks

We note that there is no need to assume the small coupling between the reservoirs and the system if the reservoirs are described as the stochastic ones and satisfy the local detailed balance (A3). It is naturally obeyed by the smallness of the heated area compared to the bulk. So, one can choose any stochastic forces of the thermostats if they keep the local detailed balance. Furthermore, these relations can be applied to the cases of the finite-size systems if it keeps the temperature gaps at the edges negligibly small.

The choice of the reference ensemble determines the accuracy of the expansion, so the reference must be chosen to keep the averages of the macroscopic variables almost unchanged under the ensemble transformation ($P^{st} \to P^{\text{ref}}$). Then, the ensemble choice of the homogeneous compression $[l_i = l, P^{\text{ref}} = \exp(-\beta_i h_i)/Z]$ would not make sense in the far from equilibriums ($\Delta\beta \sim \bar{\beta}$) in general because such a choice can allow the particles to move in average ($\partial_n P \neq 0$). Such a static steady state cannot exsist. If $\partial P(T,l)/\partial T$ becomes relevant, the difference between two ensembles is not negligible.

As a convincing example on the validity of the local equilibrium ensembles, we show the case of a thermal rectifier [65]. In that case, the system Hamiltonian takes the form

$$\mathcal{H} = \mathcal{H}_L(x_1, \ldots, x_{N_L}, p_1, \ldots, p_{N_L})$$
$$+ \mathcal{H}_R(x_{N_L+1}, \ldots, x_N, p_{N_L+1}, \ldots, p_N)$$
$$+ \lambda V(x_{N_L+1,N_L}), \lambda \ll 1. \quad (A36)$$

According to the simulation, suppose the situation

$$P = 0; \quad i \leqslant N_L, \quad T_i = T_L; \quad i > N_L, \quad T_i = T_R. \quad (A37)$$

$T_{L(R)}$ is the reservoir temperature of the left (right) side. One cannot expand Σ by $d\partial_n\beta$ now, but can get the following relation repeating the same calculation with that of Derivation 2, defining $q := j_{N_L+1,N_L}$,

$$\langle q\rangle^{st} = \Delta\beta\int dt\langle q(0)q(t)\rangle^{lc}_{\beta_L,\beta_R} + \mathcal{O}[(\Delta\beta)^2\lambda^3] \quad (A38)$$

$$\propto \lambda^2. \quad (A39)$$

$\Delta\beta := 1/T_R - 1/T_L$ is the inverse temperature difference between the left reservoir and the right reservoir. $\langle\rangle^{lc}_{\beta_L,\beta_R}$ is the average by the local equilibrium ensemble (A25) of the corresponding situation. We expanded Σ by the small parameter λ. $j_{N_L+1,N_L} \propto \lambda[dV(x_{N_L+1,N_L})]/(dx_{N_L+1,N_L}) = \mathcal{O}(\lambda)$ predicts the scaling $\langle j_{N_L+1,N_L}\rangle^{st} \propto \lambda^2$. This relation is actually observed in [65]. Also, neglecting the $\mathcal{O}(\lambda^3)$ terms in the time evolution that come from the system coupling, one can estimate the right hand side with the time evolution of the
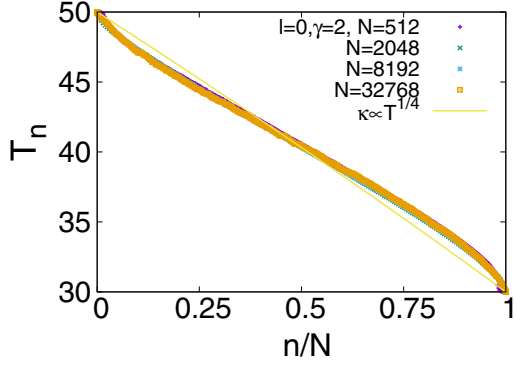
FIG. 7. Temperature profile at c-FPU β at $l = 0$, $\gamma = 2$, $T_L = 50$, $T_R = 30$ [$T_{L(R)}$: left (right) reservoir temperature]. The corresponding curve of normal heat conduction $\kappa \propto T^{1/4}$ is also shown in the same figure. There are the cusps at the edges corresponding to the anomaly but the gaps at the edges cannot be seen. The clear systematic deviation means the asymptotics of the anomaly realized in this parameter region.

FIG. 8. Temperature profile at c-FPU β at $l = 4$, $\gamma = 2$, $T_L = 50$, $T_R = 30$. The corresponding curve of normal heat conduction $\kappa \propto T^{-2.3}$ is also shown in the same figure. The clear convergence means the realization of the asymptotic form in this system. The gaps at the edges vanish at larger sizes.

separated systems ($\mathcal{H} = \mathcal{H}_L + \mathcal{H}_R$), as already done in [65]. The temperature asymmetry that cannot be treated in the expansions from the global equilibriums is now included in this linear response.

We also note that the second term in the Green Kubo of the local equilibriums (A34) would remain in the diatomic systems under the compression (tension) even if they recover the normal heat conduction. In addition, even in the case of diatomic systems around the globally equilibriums, the expansion from the isobaric equilibrium shows a different Green Kubo formula which corresponds to (A34) from the isodense case (A22). There may be another order because they should be equivalent if we specify the values of all macroscopic variables. Monatomic systems actually have no such confusion. Diatomic systems may need careful modifications on that point.

APPENDIX B: ON THE VANISHMENT OF THE TEMPERATURE GAPS AT THE EDGES

In the preceding appendix, we showed the simple derivation of the Green Kubo formula and we supposed the vanishment of the temperature gaps at the edges (between the system and the reservoirs) there. It is reasonable to have doubt whether the gaps really vanish in the simulations. We showed the data of the temperature profile only at $N = 2^{15} = 32\,768$ (Fig. 1), where the gaps still remain. Here we show the vanishment of the gaps in our simulations of c-FPU β.

We begin by seeing that the scale-invariant form of the anomaly can appear at $l = 0$ even in $\gamma = 2$, $\Delta T/\bar{T} = 0.5$. Figure 7 is the temperature profile at the parameters ($\gamma = 2$, $\Delta T/\bar{T} = 0.5$, $l = 0$). The nth particle's temperature T_n is defined by the kinetic temperature with the long time average. One can see the existence of the scale-invariant form

$$T_n = \tilde{T}_{l=0}(n/N) \tag{B1}$$

(N: system size). As is known, the heat conductivity shows power law temperature dependence $\kappa \propto T^{1/4}$ if one takes the temperature difference sufficiently small [51] in the parameter
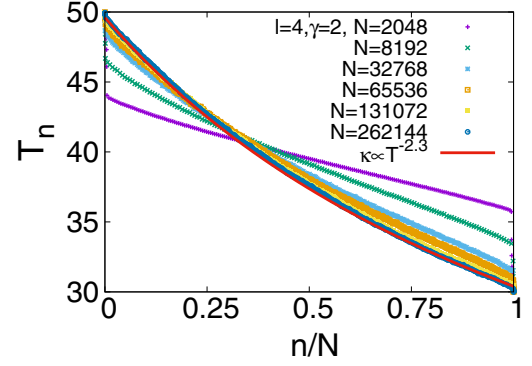
$l = 0$. If the system recovers the normal heat conduction with the power law temperature dependence of heat conductivity $\kappa \propto T^a$, their corresponding temperature profile must be described as $m \leqslant n \leqslant N - m$,

$$T_n = \left[T_{1+m}^{a+1} + \left(T_{N-m}^{a+1} - T_{1+m}^{a+1} \right) \frac{n - m}{N - 2m} \right]^{1/(a+1)}, \tag{B2}$$

but one cannot see the convergence to it in the figure (m: the number of reservoir-attached particles to each reservoir). There are increases of the gradient (cusps) around the edges (besides the gaps at the edges). This is a characteristic feature of the anomalous heat conduction and is caused by the growth of the correlation length. The position-dependent Green Kubo formula (at the position n) is proportional to $\int dt \sum_i \langle j_{n+1,n} j_{i+1,i} \rangle^{lc}$ ($\langle \rangle^{lc}$: local canonical average defined in the preceding appendix), so this is understood as the consequence of the fact that the integration range of the position becomes smaller than the correlation length ($\sim N$) [49]. Here $j_{i+1,i}$ is the energy current between the $i + 1$, ith particles. Then this systematic deviation corresponds to the anomaly. Now the temperature gaps at the edges vanish. Only the cusps remain.

Next, we checked whether the system at $l = 4$ reaches the asymptotics (Fig. 8). Before the discussion, we note that there are temperature gaps at smaller sizes, but the relation proposed by Aoki and Kusnezov (B2) [66] can be used even in these situations. Then, seeing the profile at small sizes $N = 2048, 8192, 32768$, one can find the increase of the gradient (cusps) at the edges, that corresponds to the anomaly. It means that there is actually the anomaly in this system at small sizes. The graph $\bar{\kappa} - N$ (Fig. 2) actually has the region that shows the anomaly $\bar{\kappa} \sim N^{1/3}$ and the region just corresponds to the sizes we found here. After the checking, please see the convergence to the asymptotic curve as the gaps decrease. The profile that was straight at $N = 8192$ has slowly bent and converges to the master curve $\kappa \propto T^{-2.3}$ of normal heat conduction at $N = 131\,072, 262\,144$. We put the curve of normal heat conduction $\kappa \propto T^{-2.3}$ with $T_{m+1} = 49.7$, $T_{N-m} = 30.3$. It is clear that it converges to

the profile of the normal heat conduction. At least, one can understand that this behavior is not the artifact that merely cut the preasymptotics only. The gaps vanish at larger sizes and one can safely use the Green Kubo formula in this case.

[1] S. R. De Groot and P. Mazur, *Non-equilibrium Thermodynamics* (Courier Corporation, North Chelmsford, 2013).

[2] S. Lepri, R. Livi, and A. Politi, Phys. Rep. **377**, 1 (2003).

[3] A. Dhar, Adv. Phys. **57**, 457 (2008).

[4] S. Lepri, R. Livi, and A. Politi, *Thermal Transport in Low Dimensions*, Lecture Notes in Physics Vol. 921 (Springer, Berlin, 2016), pp. 1–37.

[5] Z. Rieder, J. Lebowitz, and E. Lieb, J. Math. Phys. **8**, 1073 (1967).

[6] G. Casati, J. Ford, F. Vivaldi, and W. M. Visscher, Phys. Rev. Lett. **52**, 1861 (1984).

[7] T. Prosen and M. Robnik, J. Phys. A: Math. Gen. **25**, 3449 (1992).

[8] H. Matsuda and K. Ishii, Prog. Theor. Phys. Suppl. **45**, 56 (1970).

[9] R. J. Rubin and W. L. Greer, J. Math. Phys. **12**, 1686 (1971).

[10] A. O'Connor and J. Lebowitz, J. Math. Phys. **15**, 692 (1974).

[11] O. Narayan and S. Ramaswamy, Phys. Rev. Lett. **89**, 200601 (2002).

[12] A. Dhar, Phys. Rev. Lett. **86**, 5882 (2001).

[13] A. Kundu, A. Chaudhuri, D. Roy, A. Dhar, J. L. Lebowitz, and H. Spohn, Europhys. Lett. **90**, 40001 (2010).

[14] K. Saito and A. Dhar, Phys. Rev. Lett. **104**, 040601 (2010).

[15] H. Spohn, *Thermal Transport in Low Dimensions* (Springer, Berlin, 2016), pp. 107–158.

[16] S. Lepri, R. Livi, and A. Politi, Phys. Rev. Lett. **78**, 1896 (1997).

[17] T. Hatano, Phys. Rev. E **59**, R1 (1999).

[18] A. V. Savin, G. P. Tsironis, and A. V. Zolotaryuk, Phys. Rev. Lett. **88**, 154301 (2002).

[19] T. Mai, A. Dhar, and O. Narayan, Phys. Rev. Lett. **98**, 184301 (2007).

[20] C.-W. Chang, D. Okawa, H. Garcia, A. Majumdar, and A. Zettl, Phys. Rev. Lett. **101**, 075903 (2008).

[21] L. Landau and E. Lifshitz, *Fluid Mechanics* (Oxford University Press, New York, 1987).

[22] P. Grassberger, W. Nadler, and L. Yang, Phys. Rev. Lett. **89**, 180601 (2002).

[23] C. B. Mendl and H. Spohn, Phys. Rev. Lett. **111**, 230601 (2013).

[24] S. G. Das, A. Dhar, K. Saito, C. B. Mendl, and H. Spohn, Phys. Rev. E **90**, 012124 (2014).

[25] M. Kardar, G. Parisi, and Y.-C. Zhang, Phys. Rev. Lett. **56**, 889 (1986).

[26] C. B. Mendl and H. Spohn, J. Stat. Mech.: Theory Exp. (2015) P03007.

[27] K. Kawasaki and I. Oppenheim, Phys. Rev. **139**, A1763 (1965).

[28] Y. Pomeau and P. Resibois, Phys. Rep. **19**, 63 (1975).

[29] D. Forster, D. R. Nelson, and M. J. Stephen, Phys. Rev. A **16**, 732 (1977).

[30] T. Mai and O. Narayan, Phys. Rev. E **73**, 061202 (2006).

[31] B. Hu, B. Li, and H. Zhao, Phys. Rev. E **61**, 3828 (2000).

[32] J. Bricmont and A. Kupiainen, Phys. Rev. Lett. **98**, 214301 (2007).

[33] E. Pereira and R. Falcao, Phys. Rev. Lett. **96**, 100601 (2006).

[34] S. Lepri, R. Livi, and A. Politi, Europhys. Lett. **43**, 271 (1998).

[35] R. Kubo, M. Toda, and N. Hashitsume, *Statistical Physics II: Nonequilibrium Statistical Mechanics* (Springer Science & Business Media, New York, 2012), Vol. 31.

[36] O. V. Gendelman and A. V. Savin, Phys. Rev. Lett. **84**, 2381 (2000).

[37] C. Giardinà, R. Livi, A. Politi, and M. Vassalli, Phys. Rev. Lett. **84**, 2144 (2000).

[38] S. G. Das and A. Dhar, arXiv:1411.5247.

[39] Y. Zhong, Y. Zhang, J. Wang, and H. Zhao, Phys. Rev. E **85**, 060102(R) (2012).

[40] S. Chen, Y. Zhang, J. Wang, and H. Zhao, arXiv:1204.5933.

[41] A. V. Savin and Y. A. Kosevich, Phys. Rev. E **89**, 032102 (2014).

[42] S. G. Das, A. Dhar, and O. Narayan, J. Stat. Phys. **154**, 204 (2014).

[43] O. V. Gendelman and A. V. Savin, Europhys. Lett. **106**, 34004 (2014).

[44] L. Wang, B. Hu, and B. Li, Phys. Rev. E **88**, 052112 (2013).

[45] P. Di Cintio, R. Livi, H. Bufferand, G. Ciraolo, S. Lepri, and M. J. Straka, Phys. Rev. E **92**, 062108 (2015).

[46] S. Chen, J. Wang, G. Casati, and G. Benenti, Phys. Rev. E **90**, 032134 (2014).

[47] C. M. Newman, Commun. Math. Phys. **103**, 121 (1986).

[48] N. Bou-Rabee and H. Owhadi, SIAM J. Numer. Anal. **48**, 278 (2010).

[49] H. van Beijeren, Phys. Rev. Lett. **108**, 180601 (2012).

[50] P. I. Hurtado and P. L. Garrido, arXiv:1506.03234.

[51] K. Aoki and D. Kusnezov, Phys. Rev. Lett. **86**, 4029 (2001).

[52] G. Casati and T. Prosen, Phys. Rev. E **67**, 015203 (2003).

[53] U. Seifert, Rep. Prog. Phys. **75**, 126001 (2012).

[54] H. Eyring, J. Chem. Phys. **3**, 107 (1935).

[55] H. Spohn, J. Stat. Phys. **154**, 1191 (2014).

[56] B. Drossel and M. Kardar, Phys. Rev. B **66**, 195414 (2002).

[57] J. F. Lutsko and J. W. Dufty, Phys. Rev. E **66**, 041206 (2002).

[58] C. Kittel, *Introduction to Solid State Physics* (Wiley, New York, 2005).

[59] Y. Li, S. Liu, N. Li, P. Hänggi, and B. Li, New J. Phys. **17**, 043064 (2015).

[60] Y. A. Kosevich and A. V. Savin, arXiv:1509.03219.

[61] S. Lepri, P. Sandri, and A. Politi, Eur. Phys. J. B: Condens. Matter Complex Syst. **47**, 549 (2005).

[62] D. Bedeaux and P. Mazur, Physica **73**, 431 (1974).

[63] C. Maes and K. Netočný, J. Math. Phys. **51**, 015219 (2010).

[64] M. Itami and S.-i. Sasa, J. Stat. Phys. **158**, 37 (2015).

[65] B. Li, L. Wang, and G. Casati, Phys. Rev. Lett. **93**, 184301 (2004).

[66] K. Aoki and D. Kusnezov, Ann. Phys. **295**, 50 (2002).